Brain, Behavior, and Immunity 109 (2023) 271–284

Contents lists available at ScienceDirect

Brain Behavior and Immunity

journal homepage: www.elsevier.com/locate/ybrbi

Maternal immune activation impairs endocannabinoid signaling in the mesolimbic system of adolescent male offspring

Michele Santoni [a], Claudia Sagheddu [a], Valeria Serra [a], Rafaela Mostallino [a], Maria Paola Castelli [a], Francesco Pisano [a], Maria Scherma [a], Paola Fadda [a,b], Anna Lisa Muntoni [b], Erica Zamberletti [c], Tiziana Rubino [c], Miriam Melis [a], Marco Pistis [a,b,d,*]

[a] Department of Biomedical Sciences, Section of Neuroscience and Clinical Pharmacology, University of Cagliari, Cagliari, Italy
[b] Neuroscience Institute, Section of Cagliari, National Research Council of Italy (CNR), Cagliari, Italy
[c] Department of Biotechnology and Life Sciences and Neuroscience Center, University of Insubria, Busto Arsizio, Italy
[d] Unit of Clinical Pharmacology, University Hospital, Cagliari, Italy

ARTICLE INFO

Keywords:
Maternal immune activation
Schizophrenia
Dopamine
Endocannabinoids
Adolescence
Poly I:C

ABSTRACT

Prenatal infections can increase the risk of developing psychiatric disorders such as schizophrenia in the offspring, especially when combined with other postnatal insults. Here, we tested, in a rat model of prenatal immune challenge by the viral mimic polyriboinosinic–polyribocytidilic acid, whether maternal immune activation (MIA) affects the endocannabinoid system and endocannabinoid-mediated modulation of dopamine functions. Experiments were performed during adolescence to assess i) the behavioral endophenotype (locomotor activity, plus maze, prepulse inhibition of startle reflex); ii) the locomotor activity in response to Δ9-Tetrahydrocannabinol (THC) and iii) the properties of ventral tegmental area (VTA) dopamine neurons in vivo and their response to THC; iv) endocannabinoid-mediated synaptic plasticity in VTA dopamine neurons; v) the expression of cannabinoid receptors and enzymes involved in endocannabinoid synthesis and catabolism in mesolimbic structures and vi) MIA-induced neuroinflammatory scenario evaluated by measurements of levels of cytokine and neuroinflammation markers. We revealed that MIA offspring displayed an altered locomotor activity in response to THC, a higher bursting activity of VTA dopamine neurons and a lack of response to cumulative doses of THC. Consistently, MIA adolescence offspring showed an enhanced 2-arachidonoylglycerol-mediated synaptic plasticity and decreased monoacylglycerol lipase activity in mesolimbic structures. Moreover, they displayed a higher expression of cyclooxygenase 2 (COX-2) and ionized calcium-binding adaptor molecule 1 (IBA-1), associated with latent inflammation and persistent microglia activity. In conclusion, we unveiled neurobiological mechanisms whereby inflammation caused by MIA influences the proper development of endocannabinoid signaling that negatively impacts the dopamine system, eventually leading to psychotic-like symptoms in adulthood.

1. Introduction

The devastating effects of the ongoing pandemic of Covid-19 highlighted that infectious diseases still represent a significant concern in our society. Not only is pregnancy a significantly vulnerable period for viral infections concerning maternal health but also for the unpredictable consequences for the offspring (Allotey et al., 2020; Dashraath et al., 2020; Wastnedge et al., 2021). Mounting evidence from preclinical to clinical studies suggests a relationship between maternal immune activation (MIA) and the emergence of neurodevelopmental disorders, such as autism and schizophrenia (Allswede et al., 2020; Miller et al., 2013; Mueller et al., 2018; (U. Meyer et al., 2008; U. Meyer, 2013;Gumusoglu & Stevens, 2019; Kentner et al., 2019). Indeed, several epidemiological studies have pointed out a correlation between an imbalance in pro- and anti-inflammatory cytokine levels during pregnancy and an increased risk of developing psychosis later in life (Allotey et al., 2020; Allswede et al., 2020; Khandaker et al., 2013). Nevertheless, it should be stated that the majority of children exposed to maternal infection during prenatal life do not develop schizophrenia or related disorders. In fact, the relationship between maternal genetic factors and gene-environment

* Corresponding author Department of Biomedical Sciences, Section of Neuroscience and Clinical Pharmacology, University of Cagliari, Cagliari, Italy.
E-mail address: mpistis@unica.it (M. Pistis).

https://doi.org/10.1016/j.bbi.2023.02.002
Received 26 September 2022; Received in revised form 9 January 2023; Accepted 3 February 2023
Available online 4 February 2023

interaction plays a fundamental role in the etiology of neurodevelopmental disorders (Cheslack-Postava and Brown, 2022; Karmiloff-Smith, 2018).

One of the most characterized animal models of MIA is based on exposure during pregnancy to the polyriboinosinic-polyribocytidylic acid [poly (I:C)], a double-stranded synthetic RNA, that triggers an innate immune response by mimicking a viral infection, inducing a schizophrenia-like phenotype in the offspring (U. Meyer et al., 2005; Talukdar et al., 2020; Zuckerman et al., 2003). Indeed, offspring exposed to poly (I:C) during pregnancy showed several behavioral impairments, such as deficits in sensorimotor gating, social interaction, working memory, behavioral despair (Ding et al., 2019; Reisinger et al., 2016; Sideromenos et al., 2020). Besides, the progeny showed marked changes in brain regions key in the pathophysiology of schizophrenia, such as the ventral tegmental area (VTA), prefrontal cortex (PFC), nucleus accumbens (NAc), and hippocampus (Ito et al., 2010; U. Meyer et al., 2011; Vuillermot et al., 2010). In our previous studies, we reported sex-specific behavioral impairments in sensorimotor gating, social interaction, and memory, as well as alterations in the mesocorticolimbic pathway (De Felice et al., 2019; Luchicchi et al., 2016). Particularly, the male offspring showed a marked alteration of VTA dopamine neuron activity and a higher dopamine release in the NAc (Luchicchi et al., 2016). To verify whether a second hit could exacerbate the dysfunctions observed in adult male offspring, we treated adolescent rats with Δ9-Tetrahydrocannabinol (THC), the main psychoactive compound in cannabis (Lecca et al., 2019). Unexpectedly, THC treatment did not exacerbate the dysfunctions observed in adult rats but attenuated them. Other studies (Stollenwerk & Hillard, 2021; Aguilar et al., 2018; Gomes et al., 2015) consistently demonstrated that THC, synthetic cannabinoid receptor 1 (CB1-R) agonists or FAAH inhibitors during adolescence failed to worsen the behavioral effects observed in neurodevelopmental models of schizophrenia.

This study aimed to test the hypothesis that MIA affects the endocannabinoid system and the endocannabinoid-mediated modulation of dopamine functions. Male rats were tested during adolescence to assess (i) the behavioral endophenotype (e.g. locomotor activity, plus maze, prepulse inhibition of startle reflex); (ii) the locomotor activity in response to THC; (iii) the properties of VTA dopamine neurons in vivo and their response to cumulative doses of THC; (iv) the endocannabinoid-mediated synaptic plasticity in VTA dopamine neurons; (v) the expression of cannabinoid receptors and enzymes involved in endocannabinoid synthesis and catabolism in mesolimbic structures, and (vi) the neuroinflammatory-MIA-induced scenario evaluated by cytokine measurements and markers of neuroinflammation.

2. Methods

2.1. Animals

Female Sprague Dawley rats (Envigo, Italy) were mated at the age of 3 months. Pregnant dams on gestation day (GD) 15 were randomly assigned to treatment groups (Fig. 1). Offspring were weaned and sexed on postnatal day (PND) 21 or the day of the experiment for *ex vivo* electrophysiology. We performed all the experimental procedures on the male offspring. After weaning, offspring were housed with littermates and maintained undisturbed until experiments. Subsequently, rats were randomly assigned to the experimental procedures and care was taken to avoid assigning more than three animals from the same litter to the same experimental group. In fact, for the experiments described here, a total of 27 dams were utilized (14 were treated with vehicle and 13 with poly (I:C)). Each rat underwent only one experimental procedure, except for those tested for spontaneous locomotor activity, plus maze and prepulse inhibition. See supplementary material guidelines checklist for details.

Ex vivo electrophysiological experiments were carried out before weaning (PND 12-20) with the aim of detecting early abnormalities in dopamine neuron activity and synaptic properties. Behavioral testing started on PND 34, with a recovery period of 2 days between each testing condition in the experiment. *In vivo* electrophysiological recordings were performed at the beginning of adolescence (PND 34-36). Brains and tissues for the analysis of cannabinoid receptors, enzymes, cytokine measurements and immunoblotting for inducible cyclooxygenase 2 (COX-2), ionized calcium-binding adaptor molecule 1 (IBA-1), and glial fibrillary acidic protein (GFAP) levels were collected at PND 34-36. All procedures were performed in accordance with the European legislation EU Directive 2010/63 and were approved by the Animal Ethics Committee of the University of Cagliari and by the Italian Ministry of Health (auth. n. 658/2015-PR; 631/2020-PR).

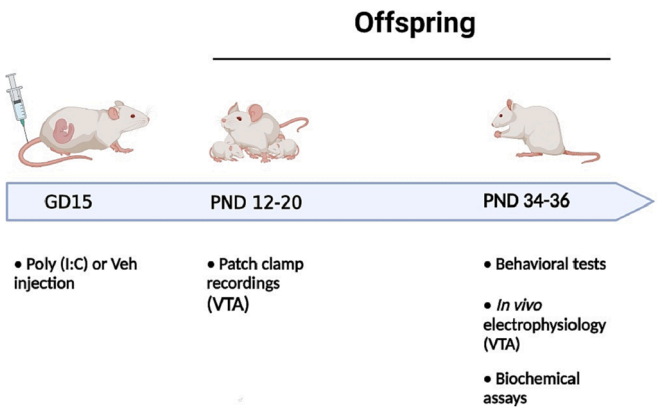

Fig. 1. Representation of the experimental protocol. Poly (I:C) treatment during pregnancy consisted of a single i.v. injection of poly (I:C) (4 mg/kg) or vehicle (sterile pyrogen-free saline) at GD15. Ex vivo electrophysiology recordings were performed between PND 12 and 20. Behavioral experiments, in vivo electrophysiology recordings and biochemical assays were performed between PND 34 and 36. Fig. 1 was created with BioRender.

2.2. Drugs and treatments

Poly (I:C) was purchased from InvivoGen. See supplementary material guidelines checklist for details. Poly (I:C) was dissolved in endotoxin-free saline solution, 4.0 mg/kg, i.v poly (I:C) was injected in the lateral vein of the tail of pregnant dams. To assess the efficacy of poly (I:C) injection, all pregnant rats were weighed for the first 3 days after the administration of either poly (I:C) or saline to evaluate weight loss, as underlined by previous investigations (Zuckerman et al., 2003). THC (THC-PharmGmbH) or vehicle (1 % ethanol, 2 % Tween 80 and saline) were injected in control and poly (I:C)-treated animals for behavioral (1.25 mg/kg and 2.5 mg/kg s.c.) and electrophysiological in vivo experiments (cumulative dose 0.3 to 2.4 mg/kg, i.v). WIN55,212–2 and JZL184 were dissolved in DMSO. The final concentration of DMSO was < 0.01 %. For cytokine measurements and immunoblotting, rats were deeply anesthetized with isoflurane (5 %) (Merial, Toulouse, France), sacrificed by decapitation, and trunk blood was collected into 5 ml tube and allowed to clot at room temperature.

2.3. Behavioral tests

2.3.1. Open field

The open field test was performed to measure spontaneous locomotor activity. Rats were recorded by a video camera to track the animal position and movements, and data were analyzed by Anymaze behavioral tracking software. The rats were individually placed in the center of a square arena (100 × 100 cm), and spontaneous motor activity was monitored for 10 min (test period). Total distance travelled (m), the number of entries into the center zone, and time spent in the center zone of the arena were scored.

2.3.2. Plus maze

The elevated plus maze test was carried out as described previously (Scherma et al, 2016). The apparatus consisted of two opposite open arms (50 × 10 cm^2) and two enclosed arms (50 × 10 × 40 cm^3) extended from a common central platform (10 × 10 cm^2). The test was performed in a room dimly illuminated by a red lamp. Rats were acclimatized to the experimental room for 30 min andthen placed in the central platform of the apparatus and video-recorded for 5 min (Ugo Basile, Any-maze). The percentage of time spent in open arms and the percentage of entries in the open arms were measured.

2.3.3. Prepulse inhibition (PPI)

On the day of the experiment, rats were placed for a 2 h period of acclimatization in the experimental room. The startle reflex system consisted of four standard cages, each placed inside a sound-attenuated and ventilated chamber (Med Associated, USA). Startle cages were non-restrictive Plexiglas cylinders (diameter 9 cm) mounted on a piezo-electric accelerometer platform connected to an analogue–digital converter. Background noise and acoustic bursts were conveyed through two speakers placed in proximity to the startle cage to produce a variation in sound intensity within 1 dB. On the test day, each rat was placed in the experimental cage for a 5-min acclimation period with a 70-dB white noise background; this was continued for the remainder of the session. Animals were then tested on three consecutive trial blocks. The first and the third blocks consisted of five pulse-alone trials of 40 ms at 115 dB, while the second block (test block) was a pseudorandom sequence of 50 trials, including 12 pulse-alone trials, 30 pulse trials preceded by 73, 76, or 82 dB prepulses (10 for each level of prepulse loudness), and eight no-stimulus trials (where the only background noise was delivered). The percentage of PPI was calculated based only on the values relative to the second block and using the following formula: 100 − [(mean startle amplitude for prepulse + pulse trials/mean startle amplitude for pulse-alone trials) × 100] (Scherma et al., 2016).

2.3.4. Locomotor activity

Rats were individually tested for locomotor sensitivity to THC using the Digiscan Animal Activity Analyzer (Omnitech Electronics, USA) in a room dimly illuminated by a neon lamp (50 Lux). The boxes were composed of transparent Plexiglas cages (42 cm × 30 cm × 60 cm) fitted with two sets of 16 photocells located at right angles to each other, projecting horizontal infrared beams 2.5 cm apart and 4 cm above the cage floor and a further set of 16 horizontal beams which height could be adapted to the size of the animals. THC (1.25 and 2.5 mg/kg) was administered s.c. in animals habituated to the activity boxes for 30 min. The total distance travelled was calculated after injection and assessed in 60 min intervals. The time course of distance travelled was recorded within 30 min before and 60 min after injection and assessed in 10 min intervals.

2.4. In vivo electrophysiology

Rats were anaesthetized with urethane 1.3 g/kg, i.p.. Rats were placed in a stereotaxic apparatus (Kopf, Tujunga, CA, USA) with their body temperature maintained at 37 ± 1 °C by a heating pad. The recording electrode was placed above the VTA (5.6–6.2 posterior to bregma, 0.4–0.8 mm lateral to the midline, 7.0–8.0 mm from the cortical surface), according to the stereotaxic rat brain atlas of Paxinos and Watson (Paxinos & Watson, 2007). Single unit activity was recorded extracellularly (bandpass filter 0.1–10,000 Hz) with glass micropipettes filled with 2 % Pontamine sky blue dissolved in 0.5 M sodium acetate. Individual action potentials were isolated and amplified through a window discriminator (Neurolog System, Digitimer, Hertfordshire, UK) and displayed on a digital storage oscilloscope (TDS 3012, Tektronics, Marlow, UK). Experiments were sampled online and offline with Spike2 software by a computer connected to CED1401 interface (Cambridge Electronic Design, Cambridge, UK). Dopamine neurons were isolated and identified according to previously described electrophysiological characteristics (Grace & Bunney, 1984; McCutcheon et al., 2012; Ungless & Grace, 2012). VTA dopamine neurons were recorded only when criteria for identification were fulfilled (firing rate 0.5–10 Hz, duration of action potential ≥ 2.5 ms). Bursts were defined as the occurrence of two spikes at interspike interval < 80 ms and terminated when the interspike interval exceeded 160 ms.

2.5. Ex vivo electrophysiology

The preparation of VTA slices was as described previously (Melis et al., 2004, 2013). Briefly, male Sprague Dawley rats (PND 12–20; Envigo) were anesthetized with isoflurane until loss of righting reflex and decapitated. Then, a block of tissue containing the midbrain was rapidly dissected and sliced in the horizontal plane (300 μm) with a vibratome (Leica) in ice-cold (4–6 °C) low-Ca2 + solution containing the following (in mM): 126 NaCl, 1.6 KCl, 1.2 NaH2PO4, 1.2 MgCl2, 0.625 CaCl2, 18 NaHCO3, and 11 glucose (300–306 mOsm). Immediately after cutting, slices were transferred to a holding chamber with artificial cerebrospinal fluid (aCSF) (37 °C) and saturated with 95 % O2 and 5 % CO2 containing the following (in mM): 126 NaCl, 1.6 KCl, 1.2 NaH2PO4, 1.2 MgCl2, 2.4 CaCl2, 18 NaHCO3, and 11 glucose (300–306 mOsm). Slices were allowed to recover for at least 1 h before being placed, as hemislices, in the recording chamber and superfused with the (aCSF) (34–36 °C) saturated with 95 % O2 and 5 % CO2. Cells were visualized with an upright microscope with infrared illumination (Axioskop FS 2 plus; Zeiss), and whole-cell patch-clamp recordings were made by using an Axopatch 200B amplifier (Molecular Devices). Voltage-clamp recordings were made with electrodes filled with a solution containing the following (in mM): 144 KCl, 10 HEPES, 3.45 BAPTA, 1 CaCl2, 2.5 Mg2ATP, and 0.25 Mg2GTP, pH 7.2–7.4, 275–285 mOsm. All GABAA IPSCs were recorded in the presence of 6-cyano-2,3-dihydroxy-7- nitroquinoxaline (10 μM) and 2-amino-5-phosphonopentanoic acid (AP5; 100 μM) to block AMPA and NMDA -receptors-mediated synaptic currents, respectively. Experiments were begun only after series resistance had stabilized (typically 10–30 MΩ). Series and input resistance were monitored continuously on-line with a 5 mV depolarizing step (25 ms). Data were filtered at 2 kHz, digitized at 10 kHz, and collected on-line with acquisition software (pClamp 10; Molecular Devices). Dopamine neurons from the lateral portion of the posterior VTA were identified according to the already published criteria (Melis et al., 2013b): cell morphology and anatomical location (i.e., medial to the medial terminal nucleus of the accessory optic tract), slow pacemaker-like firing rate (<5 Hz), long action potential duration (>2 ms), and the presence of a large hyperpolarization-activated current (Ih) (>100 pA; Johnson and North, 1992), which was assayed immediately after break-in, using 13 incremental 10 mV hyperpolarizing steps (250 ms) from a holding potential of − 70 mV. A bipolar stainless steel stimulating electrode (FHC) was placed ~100-200 μm rostral to the recording electrode and was used to stimulate at a frequency of 0.1 Hz. Paired stimuli were given with an interstimulus interval of 50 ms, and the ratio between the second and the first IPSCs (IPSC2/IPSC1) was calculated and averaged for a 5 min baseline (Melis et al., 2002). The depolarizing pulse used to evoke depolarization-induced suppression of inhibition (DSI; (Pitler & Alger, 1994) was a 500 ms to 5 s step to + 40 mV from the holding potential (Melis et al., 2004). This protocol was chosen on the evidence of an endocannabinoid tone when dopamine cells are held at + 40 mV (Melis et al., 2004). The magnitude of DSI was measured as a percentage of the mean amplitude of consecutive IPSCs after depolarization (acquired between 5 and 15 s after the end of the pulse) relative to that of 5 IPSCs before the depolarization. Bath application of WIN 55,212–2 (WIN) was performed as follows: WIN was applied for 5 min at the lowest concentration, then another 5 min with the next increasing WIN concentration. The effect of WIN on GABAA IPSCs was taken at the last minute of bath application and normalized to the baseline (5 min before drug application). We chose this protocol because it has been shown that at

physiological temperatures, WIN-induced effects on GABAA IPSCs recorded from VTA dopamine neurons reached their peak at this time. The effect of JZL (100 nM) on GABAA IPSCs was taken after 5 min bath application (Melis et al 2013, Lecca et al. 2012). Each hemislice received only a single drug exposure. All drugs were dissolved in DMSO when it was needed. The final concentration of DMSO was < 0.01 %.

2.6. Biochemical studies

2.6.1. Western Blotting: Endocannabinoid receptors and enzymes

For Western blot analysis, nucleus accumbens and midbrain were dissected, frozen in liquid nitrogen and stored at − 80∘C. Cytosolic fractions were obtained using a protocol published by (Zamberletti et al., 2019). In brief, samples were homogenized by 25 S in a glass-glass homogenizer in 0.32 M sucrose solution containing 20 mM HEPES, 1 mM MgCl2, protease inhibition cocktail, and 0.1 mM phenylmethylsulfonyl fluoride (PMSF) (pH 7.4). The homogenized tissue was centrifuged at 500 × g for 2 min. Resultant pellets (*P*1) were resuspended in 500 μL of a solution containing HEPES 20 mM, MgCl2 1.5 mM, NaCl 420 mM, EDTA 0.2 mM, glycerol 25 %, DTT 2 mM, PMSF 2 mM, protease inhibition cocktail and stored as nuclear fraction. The resulting supernatant (S1) was used as cytosolic fraction. The protein concentrations were determined according to the Micro-BCA assay kit (Pierce, Rockford, IL, United States). Equal amounts of protein lysates from the cytosolic fractions (30 μg) were run on a 10 % SDS-polyacrylamide gel. The proteins were then transferred to polyvinylidene difluoride (PVDF) membranes, blocked for 2 h at room temperature in 5 % dry skimmed milk in TBS 1×, 0.1 % tween-20 before incubation overnight at 4∘C with the primary antibody. The following primary antibodies were used: rabbit polyclonal anti-CB1 receptor (1:1000; Cayman Chemical, United States), rabbit polyclonal anti-CB2 receptor (1:1000; Cayman Chemical, United States), rabbit polyclonal anti-FAAH (1:1000; Cayman Chemical, United States), rabbit polyclonal anti-MAGL (1:1000; Cayman Chemical, United States), rabbit polyclonal anti-NAPE-PLD (1:3000; Cayman Chemical, United States), goat polyclonal anti-DAGLα (1:1000; AbCam, United Kingdom). Bound antibodies were detected with horseradish peroxidase (HRP) conjugated secondary anti-rabbit or antigoat antibodies (1:2000–5000; Santa Cruz Biotechnology, United States) for 1 h at room temperature and visualized using ECL Western Blotting Detection Reagents (Bio-Rad Laboratories, Hercules, CA, United States). To detect β-tubulin, the blots were stripped with Restore Western Blot Stripping Buffer (Thermo Scientific, Rockford, IL, United States) and re-blotted with rabbit polyclonal anti-β-tubulin (1:10000; Sigma Aldrich, United States) overnight at 4 °C and visualized as described above. Bands were detected with G-Box (Syngene) instrument. For densitometry, images were digitally scanned, and the optical density of the bands was quantified using ImageJ software (NIH, Bethesda, MD, United States) and normalized to controls. To allow comparison between different blots, the density of the bands was expressed as arbitrary units. Experiments and analysis were performed blind to treatment.

2.6.2. Western Blotting: Inflammation

Samples were thawed on ice and adjusted to a final concentration of 6 μg/μl.. Equal amounts of total proteins (30 μg) mixed with Laemmli Sample Buffer were denatured at 70 °C for 10 min and loaded on gradient gel (4–20 %, Mini-PROTEAN® TGXTM, Bio-Rad Laboratories, Inc., USA). The separated proteins were transferred onto polyvinylidene difluoride (PVDF) membranes (Amersham GE Healthcare, UK). The membranes were blocked for 1 h. at room temperature using 5 % non-fat dried milk in Tris-buffered saline containing 0.1 % Tween 20 (TBS-T) and then incubated overnight at 4 °C with the following primary antibody: mouse monoclonal anti-COX-2 (1:100; SC-376861, Santa Cruz, Dallas, Texas), rabbit polyclonal anti-Iba1 (1:1000; PA5 −27436, Invitrogen), rabbit polyclonal anti-GFAP (1:4000; Z0334, Dako, Grosschup, Denmark), mouse monoclonal anti-GAPDH (1:1000; MAB374, Sigma-Aldrich). Blots were incubated for 1 h. at room temperature with goat horseradish peroxidase (HRP) conjugated secondary anti-mouse antibody (1:10000; Jackson, PA, USA) or goat horseradish peroxidase (HRP) conjugated secondary anti-rabbit antibody (1:2000; Vector, CA, USA) and, after TBS-T washing, were incubated with the chemiluminescent detection solution Clarity Western ECL Substrate (Bio-Rad Laboratories, Inc., USA) according to the manufacturer's protocol. The intensity of immunoreactive bands was visualized by ImageQuant LAS-4000 (GE Healthcare, Little Chalfont, UK), and the density was quantified by Image Lab Software (Bio-Rad Laboratories, Inc., USA). The signal was normalized with the density of the corresponding band of endogenous protein GAPDH. Therefore, the normalized data were expressed as a protein/GAPDH ratio.

2.7. Cytokine measurements

2.7.1. Sample processing

Rats were deeply anesthetized with isoflurane (5 %), sacrificed by decapitation, and trunk blood was collected into 5 ml tubes and allowed to clot at room temperature. Then, brains were collected, the cerebellum was removed, and the whole brain minus the cerebellum was quickly snap-frozen in liquid nitrogen and stored at −80 °C. For cytokine measurements and immunoblotting for inducible COX-2, IBA-1, and GFAP tissues were prepared following the instruction of the Bio-Plex Cell Lysis Kit Product Insert.

2.7.2. Cytokine assay

Serum and brain cytokine concentrations were measured using a Luminex xMAP-based multiplex bead-based immunoassay, the Bio-Plex ProTM Rat Cytokine Group I Panel 23-Plex (Bio-Rad Laboratories, Inc., USA), which detects cytokines: [Interleukins (IL)-1α, IL-1β, IL-2, IL-4, IL-5, IL-6, IL-7, IL-10, IL-12(p70), IL-13, IL-17A, IL-18, interferon (IFN)γ, tumor necrosis factor (TNF)α; chemokines: monocyte chemotactic protein-1 (MCP-1), macrophage inflammatory protein (MIP)1α, MIP-3a, regulated on activation normal T cells expressed and secreted (RANTES), keratinocyte derived chemokine (KC/GRO/CXCL1), and growth factors: granulocytes macrophage colony-stimulating factor (GM-CSF), granulocyte (G)-CSF), macrophage (M)-CSF] and vascular endothelial growth factor (VEGF) (For details, see SI).

2.8. Statistical analysis

Data normality was preliminarily verified using the Kolmogorov-Smirnov tests for goodness of fit. Once assessed these ANOVA assumptions, we analyzed the data by one or multiway ANOVAs followed by Tukey's test for post-hoc comparisons, whenever necessary. The chi-square test and *t*-test were applied when necessary. The significance threshold was set at 0.05.

3. Results

3.1. Effects of MIA on the behavioral phenotype in MIA adolescent rats

Behavioral testing started on PND 34, with a recovery period of 2 days between each testing condition in the experiment. For this purpose, we utilized n = 8 control and n = 8 poly (I:C) male offspring. Thus, the rats were placed in the open field for 30 min of habituation; there was no significant difference between the poly (I:C) and vehicle prenatal-exposed exposed rats on distance traveled during the session (Fig. 2A) (unpaired Student's *t*-test: t(14) = 1.186, P = 0.256). Moreover, no significant group differences were found in the number of entries into the center zone (Fig. 2B) as well as in time spent in the center zone (Fig. 2C) (unpaired Student's *t*-test: t(14) = 1.275, P = 0.223 and t(14) = 1.634, P = 0.125, respectively). Furthermore, no difference was found in the percentage of open arms entries (Fig. 2D) nor in the percentage of time spent in open arms (Fig. 2E) (unpaired Student's *t*-test: t(13) =

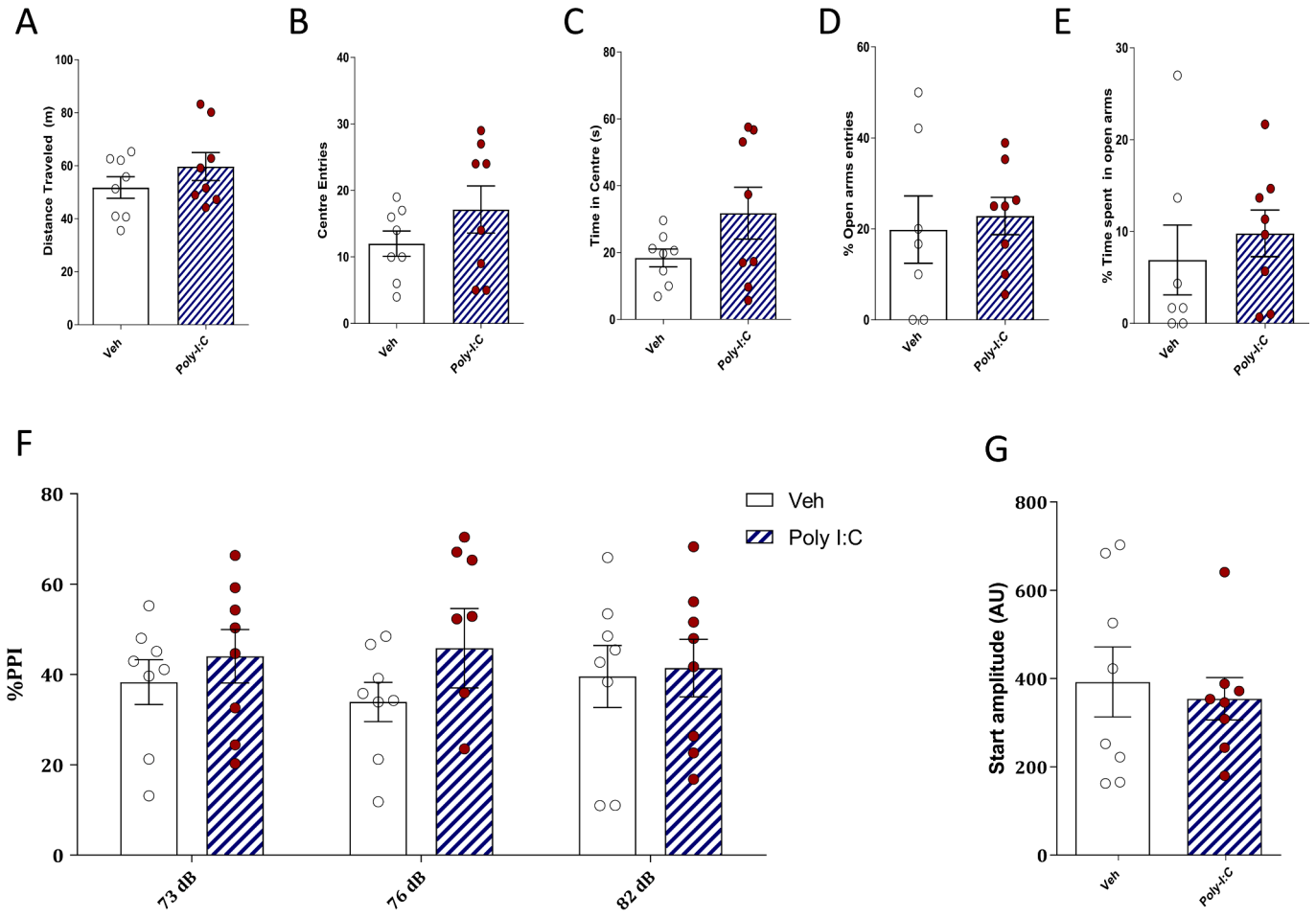

Fig. 2. Behavioral phenotype in adolescent (PND 34–36) male offspring poly (I:C) and control rats. Bar graphs in (A) show the spontaneous locomotor activity, described by the distance traveled (m) in the open field. Bar graphs in (B) display the counts of entries in the center of the open field. Bar graphs in (C) show the time (seconds) spent in the center of the open field. Bar graphs in (D) and (E) show the % of entries and the time spent in open arms, respectively. Bar graphs in (F) and (G) show the % of PPI and the startle amplitude, respectively. m, metres; s, seconds; dB, decibel; AU, arbitrary unit. Ctrl n = 8; Poly (I:C) n = 8. Data are expressed as means ± SEM. *P < 0.05.

0.367, P = 0.194 and t (13) = 0.647, P = 0.397, respectively). In addition, we assessed the prepulse inhibition of the startle reflex. In our previous studies, we observed that MIA offspring displayed disrupted PPI in adulthood (De Felice et al., 2019; Luchicchi et al., 2016). Given that during adolescence, this impairment might be latent (Ding et al., 2019), we investigated whether MIA affected PPI in adolescent male offspring. We found no significant differences between the two groups when analyzing the inhibition (PPI) of startle response at the three different prepulse intensities (two-way ANOVA treatment × prepulse interaction F(2,28) = 1.85, P = 0.176) (Fig. 2F). Moreover, control and poly (I:C) rats did not show differences in acoustic-startle response amplitude (unpaired Student's *t*-test: t(14) = 0.412, P = 0.687) (Fig. 2G).

3.2. Effects of THC on locomotor activity in MIA adolescent rats

On PND34, the rats were placed in the open field for 30 min of habituation, after which they were challenged with two different doses of THC (1.25 and 2.5 mg/kg, s.c.), and locomotor activity was monitored for 60 min (Fig. 3A). For these experiments, we used n = 14 control [7 controls tested with (1.25 mg/kg) + 7 controls tested with (2.5 mg/kg)] and n = 16 poly (I:C) male offspring [8 poly (I:C) tested with (1.25 mg/kg) + 8 tested with (2.5 mg/kg)]. Two-way ANOVA revealed an interaction between treatment with THC and poly (I:C) pretreatment (F (2,39) = 6.11, P = 0.046) and an effect of treatment with THC (F(2,39) = 6.934, P = 0.003). Post hoc analysis (Sidak test multiple comparisons) revealed a difference between poly (I:C) and control groups, revealing that THC 1.25 mg/kg s.c induced hyperlocomotion in poly (I:C) rats compared to control (Fig. 3B).

3.3. Effects of MIA and THC on dopamine cell activity and function in vivo

Since MIA altered electrophysiological properties of VTA dopamine neurons in adult male offspring but not in females (De Felice et al., 2019; Luchicchi et al., 2016), we assessed whether it might impact them during adolescence. For this purpose, we performed in vivo single-unit extracellular recordings of VTA dopamine neurons from adolescent rats under urethane anesthesia. In these experiments, we utilized n = 7 control and n = 8 poly (I:C) male offspring. Fig. 4A shows the typical broad spike waveform of a dopamine neuron, Fig. 4B depicts representative localization of recording sites of VTA putative dopamine neurons, Fig. 4C represents the classification of the VTA dopamine neurons firing pattern. Analysis of the number of cells/track (Fig. 4D), which is an index that represents the spontaneous population activity of dopamine neurons, did not reveal any difference (1.39 ± 0.07 vs 1.61 ± 0.31,

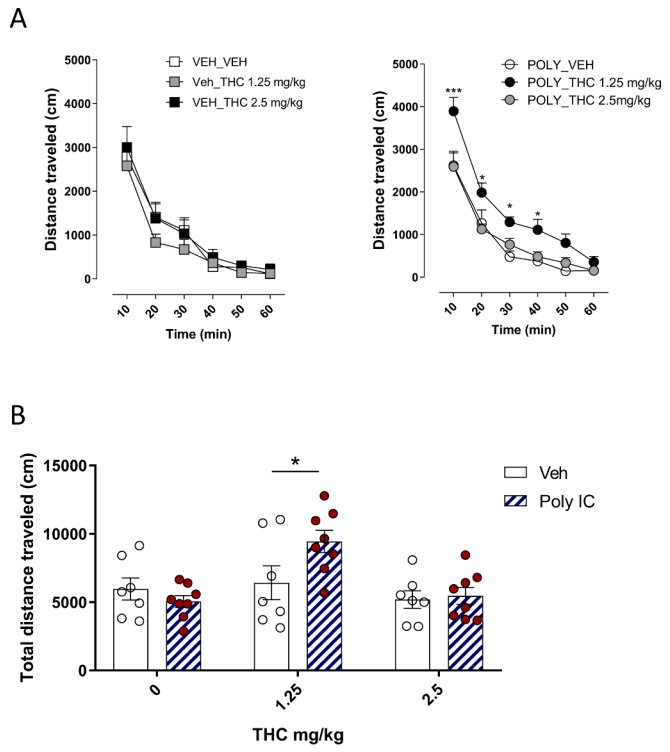

Fig. 3. Effects of THC on Locomotor Activity in MIA adolescent rats. The rats were placed in the open field for 30 min of habituation, after which they were challenged with different doses of vehicle or THC (1.25 mg/kg; 2.5 mg/kg, s.c.), and locomotor activity was monitored for 60 min (A). Bar graphs in (B) represent the total distance traveled in response to THC (0; 1,25; 2.5 mg/kg s.c.). Ctrl-Veh n = 7; Ctrl-THC n = 7; Poly (I:C)-Veh n = 8; Poly (I:C)-THC n = 8.

control vs poly (I:C); P > 0.05; Student's *t* test). Dopamine neurons recorded from control rats fired at 4.55 ± 0.17 Hz (n = 78), whereas poly (I:C) rats showed a firing frequency of 4.52 ± 0.20 Hz (n = 93); (P > 0.05. Student's *t* test) (Fig. 4E). Dopamine cells recorded from poly (I:C) presented a higher percentage of spikes in burst compared to controls (20.81 ± 2.65 %, n = 93 vs 13.47 ± 1.91 %, n = 78; (t = 2.25), P = 0.013. Student's *t* test, Welch Correction); (Fig. 4F). Consistently, autocorrelogram analysis corroborated the finding that in utero poly (I:C) treatment increases the percentage of dopamine cells showing bursting activity (37 % poly (I:C) vs 12 % control), while decreasing the percentage of regularly-firing cells (29 % poly (I:C) vs 39 % control). (p = 0.0002, Chi-Square test; Fig. 4G). We next determined whether the response of VTA dopamine neurons to cumulative doses of THC differed between groups. For these experiments, we utilized n = 6 control and n = 7 poly (I:C) male offspring. Two-way ANOVA analysis revealed an interaction between factors (poly (I:C)-pretreatment × THC-treatment) and cumulative doses of THC (from 0.3 to 2.4 mg/kg, i.v.) produced a dose-dependent decrease in the firing rate of VTA dopamine neurons in control rats whereas no effect was detected in poly (I:C) rats (Two-way ANOVA, $F_{(4, 54)} = 2.58$, P < 0.05). Post hoc analysis (Sidak test multiple comparisons) showed a difference in several points of the dose–response curve (0.6 mg/kg; 1.2 mg/kg; 2.4 mg/kg) (Fig. 4H).

3.4. Effects of MIA on endocannabinoid-mediated plasticity in vitro

The endocannabinoid system (eCBs) fine-tunes the strength of synapses in the VTA (Melis and Pistis, 2012). Therefore, the different responses of dopamine cells to THC in vivo could be ascribed to modification in endocannabinoid signaling. To test this possibility, we phasically activated eCB to elicit an endocannabinoid-mediated short-term form of synaptic plasticity termed depolarization-induced suppression inhibition (DSI) in both poly (I:C) and control groups (Diana & Marty, 2004; Pitler & Alger, 1994) (Fig. 5A). In these experiments, we utilized n = 12 control and n = 14 poly (I:C) male offspring. DSI magnitude depends on differences in 2-arachidonoylglycerol (2-AG) levels at the synapse, which are regulated by its principal degrading enzyme, i.e., monoacylglycerol lipase (MAGL) or on CB1-R number and/or function at GABAergic synapses impinging onto VTA DA neurons (Blankman et al., 2007; Di Marzo, 2011). We observed that dopamine cells from poly (I:C) offspring expressed a larger DSI when compared to controls (Fig. 5A). Next, we tested the hypothesis that this difference could be ascribed to different MAGL efficacy and/or expression. To this aim, we bath applied the potent MAGL inhibitor JZL184 (Long et al., 2009) (100 nM), or vehicle (control + vehicle n = 6 cells; poly (I:C) + vehicle n = 6 cells; control + JZL184 n = 9 cells; poly (I:C) + JZL184 n = 13 cells). In the presence of JZL184, DSI was no longer different between controls and poly (I:C) offspring. Hence, two-way ANOVA analysis revealed a significant interaction between factors (poly (I:C)-pretreatment × duration of depolarization ($F_{(9, 90)} = 2.17$, P = 0.03). Post hoc analysis (Sidak test multiple comparisons) showed a difference between Ctrl + vehicle vs poly (I:C) + vehicle (P < 0.001); Ctrl + vehicle vs Ctrl + JZL184 (P < 0.001); Ctrl + vehicle vs poly (I:C) + JZL184 (P < 0.001). No difference was observed between all other groups (Fig. 5A).

To exclude that differences in CB1-R number and/or function at GABAergic synapses impinging onto VTA DA neurons of poly (I:C) rats could contribute to different DSI magnitude, we built a dose–response relationship for CB1-R/CB2-R agonist WIN55,212–2 (WIN 0.01–3 μM). No difference was observed between the groups (Two-way ANOVA, control n = 7; poly (I:C) n = 8, $F_{(1, 13)} = 0.37$, P > 0.05) (Fig. 5B).

3.5. Effects of MIA on components of the endocannabinoid system in the mesolimbic system

We next assessed the protein levels of components of the endocannabinoid system in key brain regions of the mesolimbic system, such as the nucleus accumbens and the midbrain. In these experiments, we utilized n = 5 control and n = 5 poly (I:C) male adolescent offspring. With regard to the nucleus accumbens neither CB1-R nor CB2-R expression differed between the groups (Fig. 6) (unpaired Student *t*-test, CB1R: controls 0.472 ± 0.048, vs poly (I:C) 0.460 ± 0.035; P > 0.05; CB2-R: controls 0.394 ± 0.045, vs poly (I:C) 0.348 ± 0.068; P > 0.05). However, MIA significantly reduced MAGL expression in poly (I:C) rats compared to controls (controls 0.394 ± 0.037, vs poly (I:C) 0.207 ± 0.038; P = 0.004). Interestingly, MIA also reduced NAPE-PLD expression in poly (I:C) rats compared to controls (controls 0.149 ± 0.020, vs poly (I:C) 0.083 ± 0.009; P = 0.009). There was no significant difference between poly (I:C) and control rats neither on FAAH (controls 0.438 ± 0.0749, vs poly (I:C) 0.405 ± 0.060; P = 0.369) nor on DAGLα expression (controls 0.093 ± 0.017, vs poly (I:C) 0.142 ± 0.028, P = 0.090).

With regard to the midbrain, neither CB1-R nor CB2-R expression differed between the groups (Fig. 6) (CB1-R: unpaired Student *t*-test, controls 0.349 ± 0.050, vs poly (I:C) 0.328 ± 0.047; P > 0.05; CB2-R: controls 0.604 ± 0.094, vs poly (I:C); P > 0.05). Nevertheless, MIA significantly reduced both MAGL (controls 0.262 ± 0.034, vs poly (I:C) 0.149 ± 0.013; P = 0.075) and DAGLα expression (controls 0.212 ± 0.017, vs poly (I:C) 0.169 ± 0.011; P = 0.033) in poly (I:C) rats compared to controls. However, MIA did not affect FAAH (controls 0.457 ± 0.051, vs poly (I:C) 0.460 ± 0.012; P > 0.05) neither NAPE-PLD expression (controls 0.740 ± 0.0503, vs poly (I:C) 0.791 ± 0.057: P > 0.05) between groups.

3.6. Effects of MIA on IBA-1, GFAP, and COX-2 brain levels in adolescent rats

To determine whether MIA could induce long-lasting changes in glial cells such as astrocytes and microglia, we measured at PND35 the levels of specific neuroinflammation markers (IBA-1 and GFAP) in the total

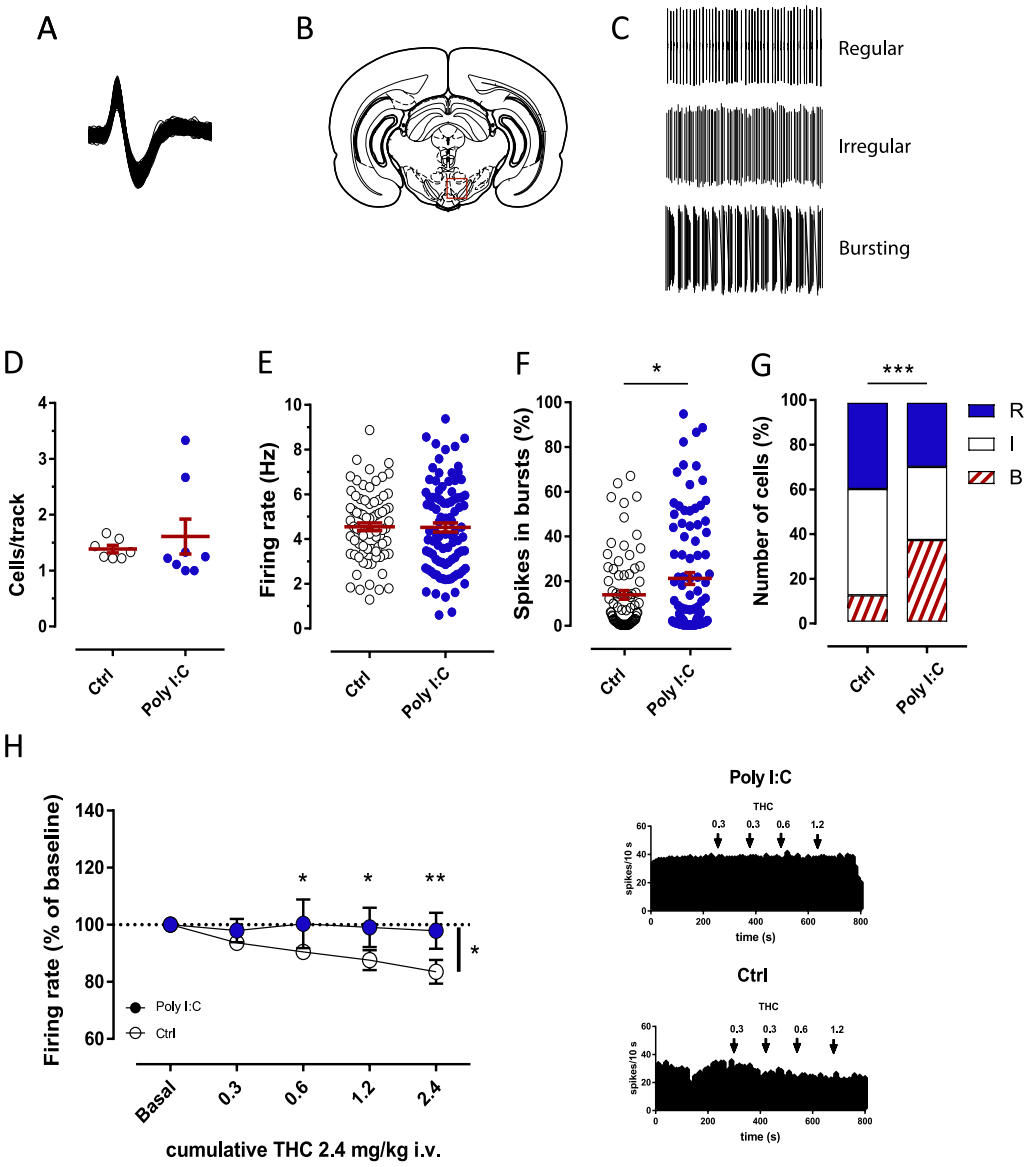

Fig. 4. MIA effects on dopamine neuron firing activity in adolescent (PND 34–46) rats. (A) The typical broad spike waveform of a dopamine neuron. (B) Representative localization of recording sites of VTA putative dopamine neurons in red, as verified by histological sections. (C) Autocorrelograms of dopamine neurons were generated from action potential recordings and allowed the classification of their firing pattern into regular (top), irregular (middle), and bursting (bottom) mode. (D) The scatter plot shows the number of spontaneously active dopamine neurons. (E) The scatter plot shows individual dopamine neuron firing rates in Ctrl and Poly (I:C) rats. The scatter plot in (F) displays individual percentages of spikes in bursts between Ctrl and Poly (I:C). Bar graphs in (G) show the percentage of cells that display a different discharge pattern. (H) On the left, cumulative THC (2.4 mg/kg i.v.) dose curve response of VTA dopamine neurons in Ctrl and Poly (I:C) adolescent rats., on the right, representative firing rate histograms of VTA dopamine neurons recorded from a Poly (I:C) (top) and Ctrl (bottom) rat. R, regular; I, irregular; B, bursting. VTA dopamine sampling: Ctrl: n = 7; Poly (I:C): n = 8; THC dose curve: Ctrl n = 6; Poly (I:C) n = 7. Data are expressed as means ± SEM. *P < 0.05.

brain of MIA- and control-offspring. In these experiments, we utilized n = 5 control and n = 5 poly (I:C) male offspring. Moreover, as microglia activation and altered function of astrocytes are often associated with another feature of inflammation, COX-2 (Cieślik et al., 2020; Zhao et al., 2022), we also investigated its expression. Fig. 7A-B, shows that both COX-2 and IBA-1 levels were significantly higher in the brain of MIA-compared with the control offspring (+30.6 % and + 40.5 %, respectively) (See Supplementary Fig. 1 for further details). Moreover, we also observed an upward trend but non-significant GFAP expression (+20 % compared with control-offspring) in MIA offspring's brain.

3.7. Effect of MIA on cytokine/chemokines/growth factor expression in the brain and serum of adolescent rats

To assess whether MIA affects the expression of chemokines, cytokines, and growth factors in the brain during adolescence, we performed a multiplex ELISA on total brain lysates and serum from control and MIA offspring at PND35. In these experiments, we utilized n = 8 control and n = 8 poly (I:C) male offspring. The levels of cytokines/chemokines and growth factors were higher in the offspring serum compared with brain lysates of both poly(I:C)- and saline-treated dams (Supplementary Table 1). Next, we compared how MIA altered the levels of chemokines/cytokines/growth factors in serum and brain lysates. As shown in Fig. 7C, in the MIA male offspring we found a significant decrease in the serum levels of GM-CSF (−16.8 %, $P < 0.05$), IFN-γ (- 32.5 %, $P < 0.05$), IL-6 (-29, $P < 0.05$) and IL-10 (-16.1 %, $P < 0.05$). Moreover, we observed a downward trend of IL-13 (30 % vs Ctrl, $P = 0.05$) in the serum, with no variations in the other cytokines/chemokines and growth factors analyzed in the serum and brain lysates (Supplementary Table 1 for details).

4. Discussion

Our results confirm that MIA perturbs the complex interplay between dopamine and endocannabinoid systems during adolescence and might generate a pathological endophenotype that leads to psychotic-like symptoms later in life. Previous work by us and others in a MIA model of schizophrenia confirmed that the dopamine function is disrupted in the adult male offspring (De Felice et al., 2019; Luchicchi et al., 2016; Vuillermot et al., 2011; Zuckerman et al., 2003), and this disruption is subsequently transmitted across generations (Weber-Stadlbauer et al., 2021; Santoni et al., 2022). THC exposure during adolescence did not exacerbate the dysfunctions observed in adult offspring but attenuated them (Lecca et al., 2019). Consistently, a recent study by Stollenwerk &

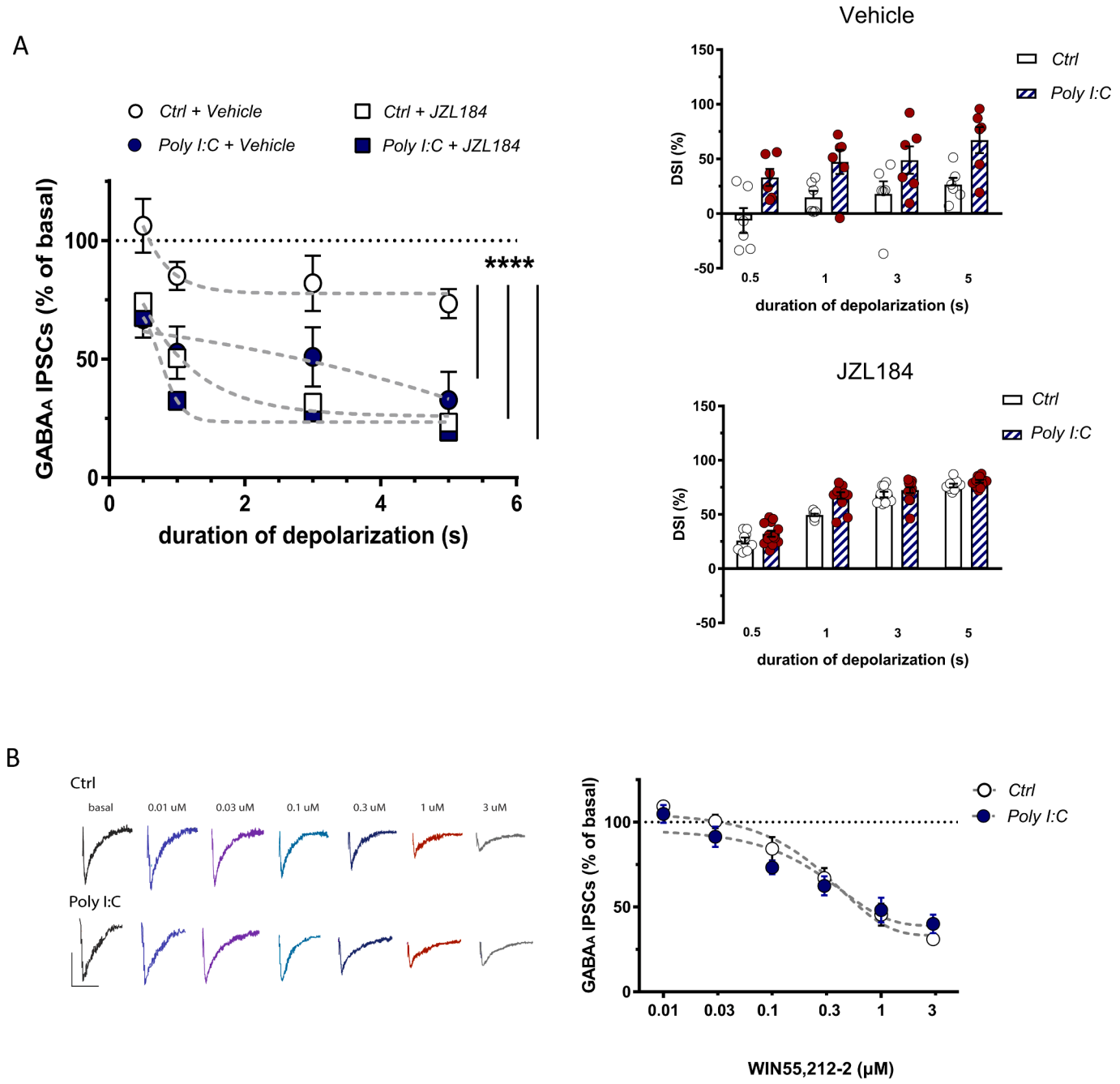

Fig. 5. MIA effects on endocannabinoid-mediated transmission *in vitro*. (A) On the left, the relationship between the depolarizing pulse duration and the relative amplitude of GABAA IPSCs obtained after the end of depolarization is plotted. GABAA IPSC amplitude was normalized to the averaged value (dotted line) before depolarization. Each symbol represents the averaged value obtained from different cells. Square symbols show ctrl and poly (I:C) groups in the presence of MAGL inhibitor JZL184. On the right, averaged data for DSI induced by depolarizing pulses with a duration of 0.5, 1, 3, and 5 s are plotted. (B) On the left, representative single traces, on the right dose–response curves for percentage inhibition of GABAA IPSCs amplitude by the CB1-R agonist WIN55,212–2 as recorded from VTA DA cells and evoked by stimulating caudal afferents. Ctrl n = 12; Poly (I:C) n = 14. ****P < 0.0001.

Hillard, 2021 confirmed our previous observations. Thus, we focused on the multifaceted interplay between the endocannabinoid and the dopamine systems and their entangled neurodevelopmental trajectories in a MIA model. We hypothesized that the inflammation caused by MIA might interfere with the development of the endocannabinoid system, which later leads to an aberrant dopamine function only in adulthood. In line with our hypothesis, the present findings revealed the persistence of long-term latent modifications in the endocannabinoid system in mesolimbic regions of adolescent male rats exposed to MIA. These modifications in poly (I:C) offspring are revealed by i) hyperlocomotion induced by a THC challenge; ii) increased bursting activity of dopamine cells; iii) larger 2-AG-mediated DSI; iv) decreased expression of MAGL; v) different effect of THC administration on the firing activity of dopamine cells. In spite of these latent changes in the endocannabinoid system, adolescent offspring in MIA models did not display behavioral disruption. Here we confirmed that sensorimotor gating, one of the core behavioral correlates of schizophrenia, is not altered during adolescence (Ding et al., 2019). In contrast, behavioral disruption is evident during adulthood (De Felice et al., 2019; Luchicchi et al., 2016). Consistently, while there was no significant difference between poly (I:C) and control rats on spontaneous locomotor activity, a THC challenge induced hyperlocomotion only in poly (I:C) offspring, suggesting a hidden

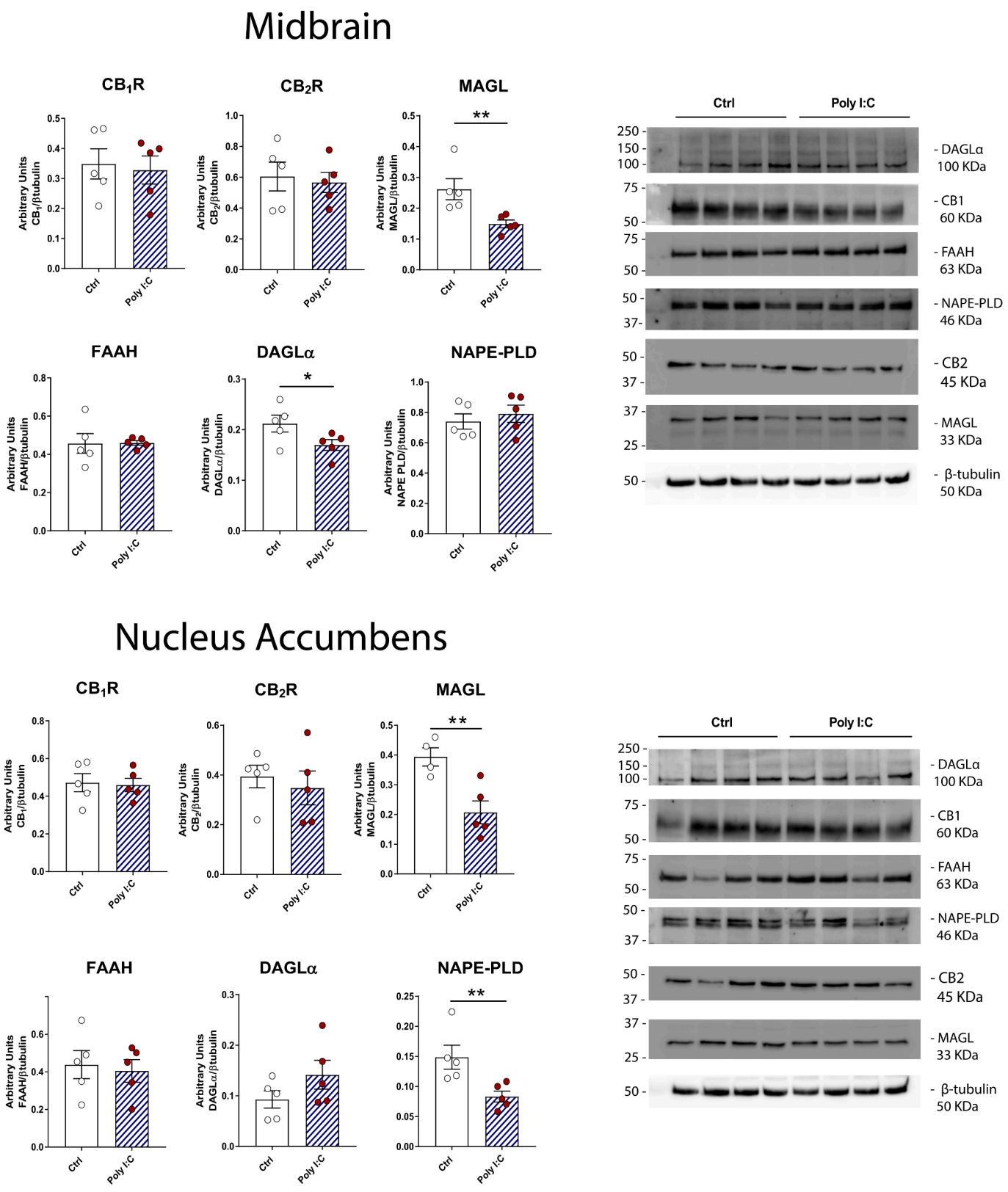

Fig. 6. Effect of MIA on components of the endocannabinoid system in the midbrain and in the nucleus accumbens of the adolescent (PND 34–36) male offspring rats measured by means of Western blot analysis in cytosolic fractions. On the right, representative immunoblot related to the protein expression levels of DAGLα (100 kDa), CB1 receptor (60 kDa), FAAH (63 kDa), NAPE-PLD (46 kDa), CB2 receptor (45 kDa), MAGL (33 kDa), and β-tubulin (50 kDa) in the midbrain (top) and in the NAc (bottom) homogenates of controls (n = 5) and poly (I:C) treated rats (n = 5). Data represent mean ± SEM. *P < 0.05.

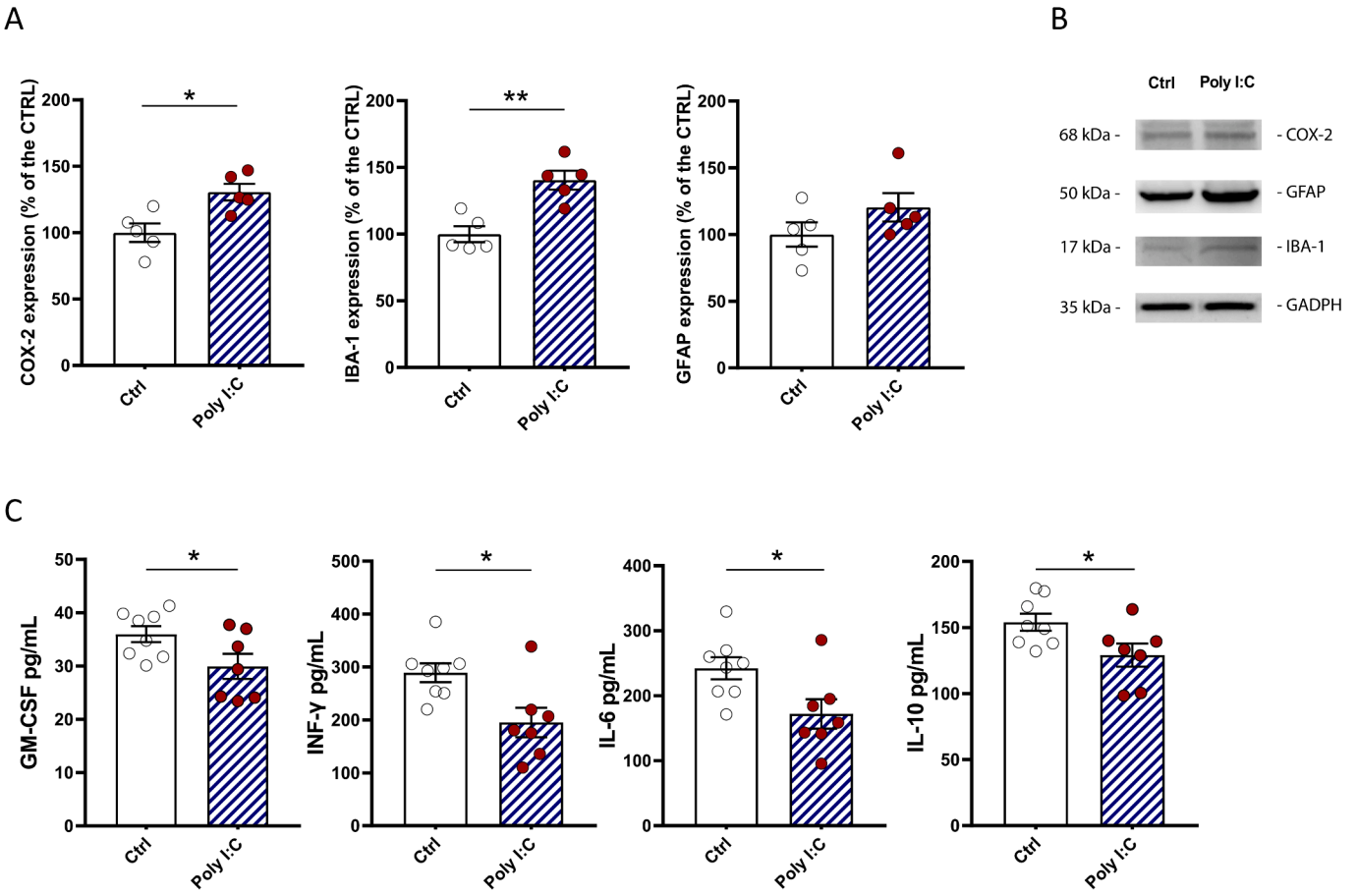

Fig. 7. Effect of MIA on cytokine/chemokines/growth factor expression in the brain and serum of adolescent rats. (A) On the left, the bar graph shows COX-2 expression, in the middle IBA-1 expression, on the right GFAP expression. The protein levels of COX-2, IBA-1, and GFAP were quantified and normalized to loading control GADPH. Values represent mean ± SEM of COX-2, IBA-1, and GFAP levels expressed as a percentage of Ctrl normalized to GAPDH. (B) Representative illustration of Western blotting analysis. (C) On the left, the bar graph shows GM-CSF expression, in the middle INF-γ and IL-6 expression, on the right IL-10 expression. Data are expressed as mean ± SEM for each growth factor/cytokine, expressed as pg/ml. Ctrl n = 8; Poly (I:C) n = 8. Data represent mean ± SEM. *P < 0.05.

impairment of the endocannabinoid system that resurfaces only after the THC administration. A similar scenario is revealed when considering the VTA dopamine neuron activity. In fact, there are no differences between groups in basal firing frequency nor in the cells per track during adolescence, whereas MIA animals displayed a disrupted VTA dopamine neuron activity in adulthood (Luchicchi et al., 2016). However, MIA adolescent rats showed a bursting activity higher than controls, the opposite of what we observed in adulthood (Luchicchi et al., 2016). Moreover, cumulative doses of THC inhibited VTA dopamine cells in control animals, whereas in MIA offspring, they were unresponsive. This observation is in contrast with the scenario observed in adult control rats, where cannabinoids increase the firing rate of VTA dopamine neurons (French, 1997; Gessa et al., 1998; Wu & French, 2000). There are several possible explanations: i) an incomplete maturation of the excitatory and inhibitory inputs to the VTA DA neurons; ii) a different expression of CB1-R between adolescence and adulthood (H. C. Meyer et al., 2018) and/or iii) altered 2-AG signaling in the mesolimbic pathway. In line with our hypothesis, MIA offspring displayed a larger 2-AG-mediated DSI than controls. The larger DSI in poly (I:C) rats was not due to differences in CB1-R number or function but to a reduced 2-AG degradation. These results provide further evidence that 2-AG is a key player of DSE/DSI in the VTA (Melis & Pistis, 2007; Melis et al., 2013, 2014). Consistently, poly (I:C) rats showed a decreased level of MAGL, the enzyme that hydrolyzes 2-AG, both in the nucleus accumbens and midbrain. Poly (I:C) animals also displayed a decreased expression of DAGLα in the midbrain, which could be explained as an adaptation to an excessive 2-AG tone due to reduced MAGL expression both in the midbrain and nucleus accumbens. Remarkably, several animal models of psychiatric diseases that use different prenatal insults showed an altered endocannabinoid-mediated synaptic plasticity, and enhanced 2-AG signaling in mesolimbic structures, suggesting a common altered pathway that eventually leads to a neurodevelopmental impairment (Castelli et al., 2007; Frau et al., 2019; Melis et al., 2014). One limitation is that patch-clamp experiments were carried out on younger rats, when compared to the other experiments, due to technical reasons. However, the finding of an altered endocannabinoid function is consistently reported.

Hence, it should be pointed out that 2-AG exerts anti-inflammatory effects through CB1-R/CB2-R and, possibly, via peroxisome proliferator-activated receptor (PPAR) (Alhouayek et al., 2014). Given that 2-AG has been considered to play the role of ‘reservoir’ for arachidonic acid production by cells under inflammatory conditions (Alhouayek et al., 2014), we could speculate that enhanced 2-AG levels are an adaptive process to increased proinflammatory cytokines levels caused by MIA. Consistently, 2-AG inhibits proinflammatory cytokine production in lipopolysaccharide-activated cultures of rat microglial cells, murine splenocytes peritoneal macrophages and exhibits anti-proliferative effects toward lymphocytes (Facchinetti et al., 2003; Gallily et al., 2000; Lourbopoulos et al., 2011; Rockwell et al., 2006). On the other hand, an imbalance in 2-AG levels triggers an altered

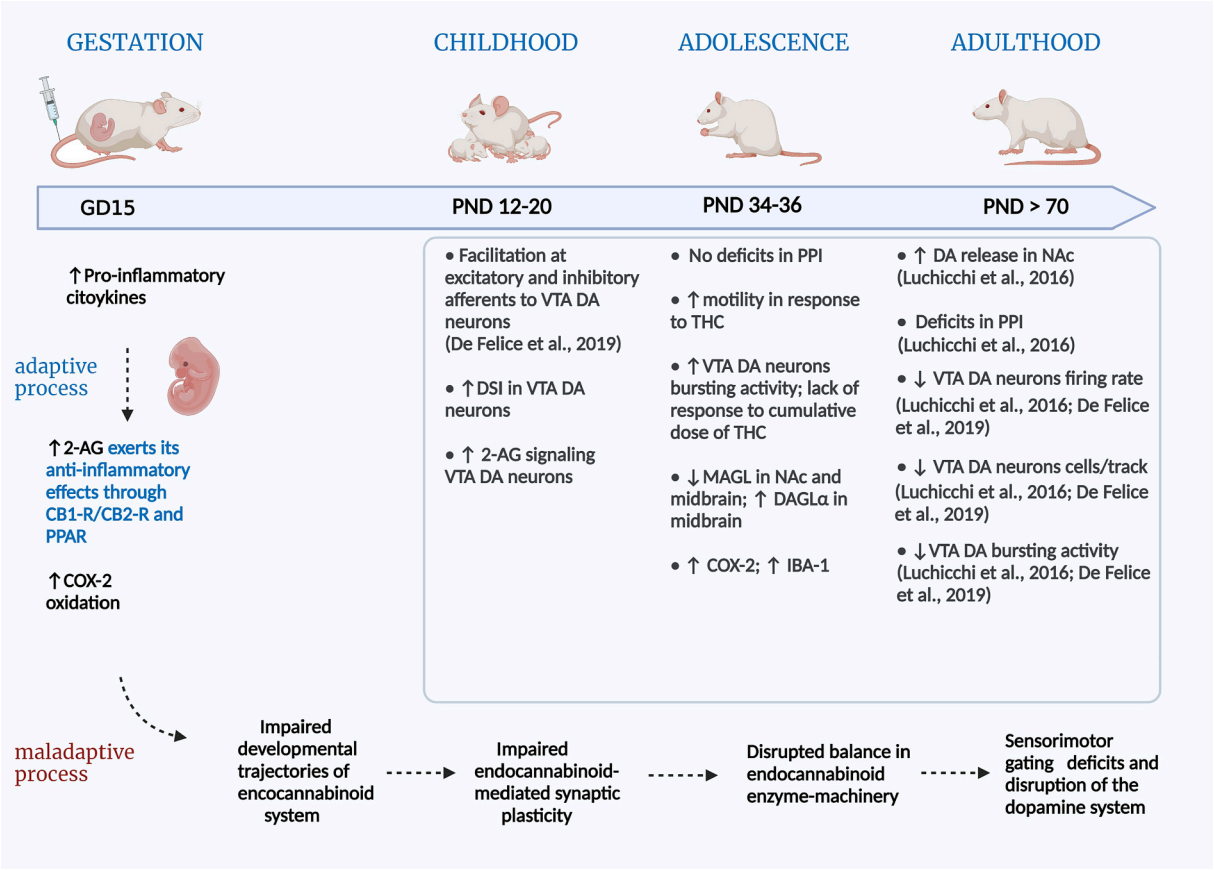

Fig. 8. Representation of the hypothesized mechanisms of the neurodevelopmental trajectories in a MIA model of schizophrenia. Fig. 8 was created with BioRender.

endocannabinoid-mediated synaptic plasticity in mesolimbic structures, eventually leading to a disrupted dopamine system in adulthood, resembling a schizophrenia-like endophenotype (Fig. 8).

Furthermore, MIA induces an increase in microglial density in the brains of neonatal, adolescent mouse offspring (Juckel et al., 2011), neonatal and adult rat offspring (Girard et al., 2010; Van Den Eynde et al., 2014). Additionally, enhanced astrocyte density, activation, and elevated GFAP mRNA expression occur in adolescent to adult rat offspring (de Souza et al., 2015; Samuelsson et al., 2006). Accordingly, here we demonstrate in the brain of adolescent MIA offspring an upward trend of GFAP and a significant increase of IBA-1, which was associated with the rise of COX-2. Among many inflammatory factors found during neuroinflammation, inducible COX-2 is a critical enzyme expressed in response to cytokines and proinflammatory mediators. Malkova and colleagues (Malkova et al., 2014) have found increased COX-2 in mouse frontal cortex in a poly(I:C) MIA model, and here we displayed the increased expression of COX-2 in the adolescent MIA brains. Moreover, COX-2 is implicated in 2-AG degradation (López & Ballaz, 2020; Luchicchi & Pistis, 2012); thus, COX-2 increased expression could be an adaptation to 2-AG enhanced levels (Fig. 8. With regard to the effect of MIA on cytokines/chemokines, a few studies, most of them performed in mice, reported postnatal brain or peripheral cytokine abnormalities following in utero poly (I:C) challenge (Giovanoli et al., 2016; Clark et al., 2019; Sullivan et al., 2006). Although there is a consensus on a proinflammatory effect during postnatal development, the results are conflicting, as other studies report no signs of inflammation in offspring born to immune-challenged mothers (Missault et al., 2014; Willi et al., 2013), or even a reduction in inflammatory cytokines in the periphery (Pacheco-López et al., 2013). These discrepancies might be attributed to several factors such as different strains and rodent species, doses, route of administration of poly (I:C), gestational time of injection, age of outcome assessment (prenatal, pre-weaning, post-weaning), and sampling utilized (blood, brain). Here, in agreement with other groups (Pacheco-López et al., 2013), we demonstrated a significant decrease in serum levels of the proinflammatory cytokines IL-6 in adolescent rats. By contrast, Garay and colleagues (Garay et al., 2013) reported that IL-6 and IL1α levels are higher in MIA mice offspring compared to controls at PND30. We also observed a downward trend in IL-13 and a significant decrease in GM-CSF and IL-10, the latter being the best-known anti-inflammatory cytokines. Indeed, IL-10, primarily due to its ability to selectively suppress proinflammatory gene transcription in activated macrophages (Lang et al., 2002), selectively blocks the expression of proinflammatory genes encoding cytokines, chemokines, and other molecules involved in the propagation of inflammation (Fiorentino et al., 1991; Murray, 2006, Moore et al., 2016). Regarding IL-13, this is a cytokine derived from T cells that selectively induces cell death of activated microglia (Shin et al., 2004; Yang et al., 2002) and displays anti-inflammatory properties, such as inhibition of the production of other inflammatory cytokines (IL-1α, IL-1β, IL-6), through its action on macrophages.

A limitation of this study is the absence of information about cytokines levels in specific brain areas such as nucleus accumbens, midbrain, and striatum. Therefore, further studies are needed to determine the importance of neuroinflammatory patterns in selected brain areas.

It remains to be established the mechanism whereby activation of the endocannabinoid system during adolescence leads to attenuation of the effects of MIA. One possibility is that CB1-R agonists might suppress TLR3 and TLR4 signaling. Hence, it has been shown that the synthetic WIN55,212–2 acts on TLR3 and TLR4 signaling by inhibiting the proinflammatory signaling pathway triggered by TLR3 and TLR4, whereas selectively augmenting TLR3-induced activation of interferon (IFN) regulatory factor 3 and expression of IFN-β (Downer et al., 2011).

The other possibility is that CB2-R are involved (Rom & Persidsky, 2013). Indeed, it has been shown that CB2-R activation decreased IL-1β, IL-6 levels and inhibited the release of TNFα in microglia (Facchinetti et al., 2003; Ramírez et al., 2005).

5. Conclusions

There is neat evidence that MIA could interfere with the physiological neurodevelopmental trajectories in the offspring. Our findings, in line with other neurodevelopmental models (Castelli et al., 2007; Frau et al., 2019; Melis et al., 2014), support the hypothesis that a prenatal insult might impair the correct development of the endocannabinoid system, ultimately leading to an altered dopamine system, unmasking latent pathological phenotype. Further investigation and evaluation of several early time points (e.g. postnatal period and childhood vs adolescence and adulthood) might provide new insight into the timing of early changes, key in preventing later abnormalities. In conclusion, the present findings contribute to unveil the neurobiological mechanisms whereby inflammation caused by MIA influences endocannabinoid signaling, which negatively impacts on the dopamine system eventually leading to psychotic-like symptoms in adulthood.

Funding

This work was supported by "FSC 2014–2020—Patto per lo Sviluppo della Regione Sardegna, Legge Regionale n. 7 del 7 agosto 2007 (Bando 2017)", by "Progetti di Rilevante Interesse Nazionale" (PRIN) 2017 (2017YH3SXK) and by a grant, with the code POC01_00069 from the Italian Ministry of University and Research (MUR) within the program Proof of Concept.

Declaration of Competing Interest

The authors declare that they have no known competing financial interests or personal relationships that could have appeared to influence the work reported in this paper.

Data availability

Data will be made available on request.

Acknowledgement

We thank Marta Tuveri and Dr. Barbara Tuveri for their skillful assistance.

Appendix A. Supplementary data

Supplementary data to this article can be found online at https://doi.org/10.1016/j.bbi.2023.02.002.

References

Aguilar, D.D., Giuffrida, A., Lodge, D.J., 2018. Adolescent Synthetic Cannabinoid Exposure Produces Enduring Changes in Dopamine Neuron Activity in a Rodent Model of Schizophrenia Susceptibility. Int. J. Neuropsychopharmacol. 21 (4), 393–403. https://doi.org/10.1093/ijnp/pyy003.

Alhouayek, M., Masquelier, J., Muccioli, G.G., 2014. Controlling 2-arachidonoylglycerol metabolism as an anti-inflammatory strategy. Drug Discov. Today 19 (3), 295–304. https://doi.org/10.1016/j.drudis.2013.07.009.

Allotey, J., Stallings, E., Bonet, M., Yap, M., Chatterjee, S., Kew, T., Debenham, L., Llavall, A. C., Dixit, A., Zhou, D., Balaji, R., Lee, S. I., Qiu, X., Yuan, M., Coomar, D., Van Wely, M., Van Leeuwen, E., Kostova, E., Kunst, H., … Thangaratinam, S. (2020). Clinical manifestations, risk factors, and maternal and perinatal outcomes of coronavirus disease 2019 in pregnancy: Living systematic review and meta-analysis. *The BMJ*, *370*. https://doi.org/10.1136/bmj.m3320.

Allswede, D.M., Yolken, R.H., Buka, S.L., Cannon, T.D., 2020. Cytokine concentrations throughout pregnancy and risk for psychosis in adult offspring: a longitudinal case-control study. Lancet Psychiatry 7 (3), 254–261. https://doi.org/10.1016/S2215-0366(20)30006-7.

Blankman, J.L., Simon, G.M., Cravatt, B.F., 2007. A Comprehensive Profile of Brain Enzymes that Hydrolyze the Endocannabinoid 2-Arachidonoylglycerol. Chem. Biol. 14 (12), 1347–1356. https://doi.org/10.1016/j.chembiol.2007.11.006.

Castelli, M.P., Paola Piras, A., D'Agostino, A., Pibiri, F., Perra, S., Gessa, G.L., Maccarrone, M., Pistis, M., 2007. Dysregulation of the endogenous cannabinoid system in adult rats prenatally treated with the cannabinoid agonist WIN 55,212–2. Eur. J. Pharmacol. 573 (1–3), 11–19. https://doi.org/10.1016/j.ejphar.2007.06.047.

Cheslack-Postava, K., Brown, A.S., 2022. Prenatal infection and schizophrenia: A decade of further progress. Schizophr. Res. 247, 7–15.

Cieślik, M., Gąssowska-Dobrowolska, M., Jęśko, H., Czapski, G.A., Wilkaniec, A., Zawadzka, A., Dominiak, A., Polowy, R., Filipkowski, R.K., Boguszewski, P.M., Gewartowska, M., Frontczak-Baniewicz, M., Sun, G.Y., Beversdorf, D.Q., Adamczyk, A., 2020. Maternal immune activation induces neuroinflammation and cortical synaptic deficits in the adolescent rat offspring. Int. J. Mol. Sci. 21 (11), 1–29. https://doi.org/10.3390/ijms21114097.

Clark, S.M., Notarangelo, F.M., Li, X., Chen, S., Schwarcz, R., Tonelli, L.H., 2019. Maternal immune activation in rats blunts brain cytokine and kynurenine pathway responses to a second immune challenge in early adulthood. Prog. Neuropsychopharmacol. Biol. Psychiatry 89 (June 2018), 286–294. https://doi.org/10.1016/j.pnpbp.2018.09.011.

Dashraath, P., Wong, J.L.J., Lim, M.X.K., Lim, L.M., Li, S., Biswas, A., Choolani, M., Mattar, C., Su, L.L., 2020. Coronavirus disease 2019 (COVID-19) pandemic and pregnancy. Am. J. Obstet. Gynecol. 222 (6), 521–531. https://doi.org/10.1016/j.ajog.2020.03.021.

De Felice, M., Melis, M., Aroni, S., Muntoni, A.L., Fanni, S., Frau, R., Devoto, P., Pistis, M., 2019. The PPARα agonist fenofibrate attenuates disruption of dopamine function in a maternal immune activation rat model of schizophrenia. CNS Neurosci. Ther. 25 (5), 549–561.

Di Marzo, V., 2011. Endocannabinoid signaling in the brain: Biosynthetic mechanisms in the limelight. Nat. Neurosci. 14 (1), 9–15. https://doi.org/10.1038/nn.2720.

Diana, M.A., Marty, A., 2004. Endocannabinoid-mediated short-term synaptic plasticity: Depolarization-induced suppression of inhibition (DSI) and depolarization- induced suppression of excitation (DSE). Br. J. Pharmacol. 142 (1), 9–19. https://doi.org/10.1038/sj.bjp.0705726.

Ding, S., Hu, Y., Luo, B., Cai, Y., Hao, K., Yang, Y., Zhang, Y., Wang, X., Ding, M., Zhang, H., Li, W., Lv, L., 2019. Age-related changes in neuroinflammation and prepulse inhibition in offspring of rats treated with Poly I: C in early gestation. Behav. Brain Funct. 15 (1), 1–10. https://doi.org/10.1186/s12993-019-0154-2.

Downer, E.J., Clifford, E., Gran, B., Nel, H.J., Fallon, P.G., Moynagh, P.N., 2011. Identification of the synthetic cannabinoid R(+)WIN55,212–2 as a novel regulator of IFN regulatory factor 3 activation and IFN-β expression: Relevance to therapeutic effects in models of multiple sclerosis. J. Biol. Chem. 286 (12), 10316–10328. https://doi.org/10.1074/jbc.M110.188599.

Facchinetti, F., Del Giudice, E., Furegato, S., Passarotto, M., Leon, A., 2003. Cannabinoids ablate release of TNFα in rat microglial cells stimulated with lypopolysaccharide. Glia 41 (2), 161–168. https://doi.org/10.1002/glia.10177.

Frau, R., Miczán, V., Traccis, F., Aroni, S., Pongor, C.I., Saba, P., Serra, V., Sagheddu, C., Fanni, S., Congiu, M., Devoto, P., Cheer, J.F., Katona, I., Melis, M., 2019. Prenatal THC exposure produces a hyperdopaminergic phenotype rescued by pregnenolone. Nat. Neurosci. 22 (12), 1975–1985. https://doi.org/10.1038/s41593-019-0512-2.

French, E.D., 1997. Δ9-Tetrahydrocannabinol excites rat VTA dopamine neurons through activation of cannabinoid CB1 but not opioid receptors. Neurosci. Lett. 226 (3), 159–162. https://doi.org/10.1016/S0304-3940(97)00278-4.

Gallily, R., Breuer, A., Mechoulam, R., 2000. 2-Arachidonylglycerol, an endogenous cannabinoid, inhibits tumor necrosis factor-α production in murine macrophages, and in mice. Eur. J. Pharmacol. 406 (1), 1997–1999. https://doi.org/10.1016/S0014-2999(00)00653-1.

Garay, P.A., Hsiao, E.Y., Patterson, P.H., McAllister, A.K., 2013. Maternal immune activation causes age- and region-specific changes in brain cytokines in offspring throughout development. Brain Behav. Immun. 31, 54–68. https://doi.org/10.1016/j.bbi.2012.07.008.

Gessa, G., Melis, M., Muntoni, A., Diana, M., 1998. Cannabinoids activate mesolimbic dopamine neurons by an action on cannabinoid CB1 receptors. Eur. J. Pharmacol. 341 (1), 39–44. https://doi.org/10.1016/S0014-2999(97)01442-8.

Giovanoli, S., Weber-Stadlbauer, U., Schedlowski, M., Meyer, U., Engler, H., 2016. Prenatal immune activation causes hippocampal synaptic deficits in the absence of overt microglia anomalies. Brain Behav. Immun. 55, 25–38. https://doi.org/10.1016/j.bbi.2015.09.015.

Girard, S., Tremblay, L., Lepage, M., Sébire, G., 2010. IL-1 Receptor Antagonist Protects against Placental and Neurodevelopmental Defects Induced by Maternal Inflammation. J. Immunol. 184 (7), 3997–4005.

Gomes, F.V., Guimaraes, F.S., Grace, A.A., 2015. Effects of pubertal cannabinoid administration on attentional set-shifting and dopaminergic hyper-responsivity in a developmental disruption model of schizophrenia. Int. J. Neuropsychopharmacol. 18 (2), 1–10. https://doi.org/10.1093/ijnp/pyu018.

Grace, A. A., & Bunney, B. S. (1984). The control of firing pattern in nigral dopamine neurons: single spike firing. *The Journal of Neuroscience*, *4*(11), 2866–2876. https://doi.org/6150071.

Gumusoglu, S.B., Stevens, H.E., 2019. Maternal Inflammation and Neurodevelopmental Programming: A Review of Preclinical Outcomes and Implications for Translational Psychiatry. Biol. Psychiatry 85 (2), 107–121. https://doi.org/10.1016/j.biopsych.2018.08.008.

Ito, H.T., Smith, S.E.P., Hsiao, E., Patterson, P.H., 2010. Maternal immune activation alters nonspatial information processing in the hippocampus of the adult offspring. Brain Behav. Immun. 24 (6), 930–941. https://doi.org/10.1016/j.bbi.2010.03.004.

Juckel, G., Manitz, M.P., Brüne, M., Friebe, A., Heneka, M.T., Wolf, R.J., 2011. Microglial activation in a neuroinflammational animal model of schizophrenia - a pilot study. Schizophr. Res. 131 (1–3), 96–100. https://doi.org/10.1016/j.schres.2011.06.018.

Karmiloff-Smith, A. (2018). Development itself is the key to understanding developmental disorders. *Thinking Developmentally from Constructivism to Neuroconstructivism: Selected Works of Annette Karmiloff-Smith*, *2*(10), 97–117. https://doi.org/10.4324/9781315516691-5.

Kentner, A.C., Bilbo, S.D., Brown, A.S., Hsiao, E.Y., McAllister, A.K., Meyer, U., Pearce, B. D., Pletnikov, M.V., Yolken, R.H., Bauman, M.D., 2019. Maternal immune activation: reporting guidelines to improve the rigor, reproducibility, and transparency of the model. Neuropsychopharmacology 44 (2), 245–258. https://doi.org/10.1038/s41386-018-0185-7.

Khandaker, G.M., Zimbron, J., Lewis, G., Jones, P.B., 2013. Prenatal maternal infection, neurodevelopment and adult schizophrenia: A systematic review of population-based studies. Psychol. Med. 43 (2), 239–257. https://doi.org/10.1017/S0033291712000736.

Lang, R., Patel, D., Morris, J.J., Rutschman, R.L., Murray, P.J., 2002. Shaping Gene Expression in Activated and Resting Primary Macrophages by IL-10. J. Immunol. 169 (5), 2253–2263.

Lecca, S., Melis, M., Luchicchi, A., Muntoni, A.L., Pistis, M., 2012. Inhibitory inputs from rostromedial tegmental neurons regulate spontaneous activity of midbrain dopamine cells and their responses to drugs of abuse. Neuropsychopharmacology 37 (5), 1164–1176. https://doi.org/10.1038/npp.2011.302.

Lecca, S., Luchicchi, A., Scherma, M., Fadda, P., Muntoni, A.L., Pistis, M., 2019. Δ9-Tetrahydrocannabinol During Adolescence Attenuates Disruption of Dopamine Function Induced in Rats by Maternal Immune Activation. Front. Behav. Neurosci. 13 (September), 1–8. https://doi.org/10.3389/fnbeh.2019.00202.

Long, J.Z., Li, W., Booker, L., Burston, J.J., Kinsey, S.G., Schlosburg, J.E., Pavón, F.J., Serrano, A.M., Selley, D.E., Loren, H., Lichtman, A.H., Cravatt, B.F., 2009. HHS Public Access. 5 (1), 37–44. https://doi.org/10.1038/nchembio.129.Selective.

López, D.E., Ballaz, S.J., 2020. The Role of Brain Cyclooxygenase-2 (Cox-2) Beyond Neuroinflammation: Neuronal Homeostasis in Memory and Anxiety. Mol. Neurobiol. 57 (12), 5167–5176. https://doi.org/10.1007/s12035-020-02087-x.

Lourbopoulos, A., Grigoriadis, N., Lagoudaki, R., Touloumi, O., Polyzoidou, E., Mavromatis, I., Tascos, N., Breuer, A., Ovadia, H., Karussis, D., Shohami, E., Mechoulam, R., Simeonidou, C., 2011. Administration of 2-arachidonoylglycerol ameliorates both acute and chronic experimental autoimmune encephalomyelitis. Brain Res. 1390, 126–141. https://doi.org/10.1016/j.brainres.2011.03.020.

Luchicchi, A., Lecca, S., Melis, M., De Felice, M., Cadeddu, F., Frau, R., Muntoni, A.L., Fadda, P., Devoto, P., Pistis, M., 2016. Maternal immune activation disrupts dopamine system in the offspring. Int. J. Neuropsychopharmacol. 19 (7), 1–10. https://doi.org/10.1093/ijnp/pyw007.

Luchicchi, A., Pistis, M., 2012. Anandamide and 2-arachidonoylglycerol: Pharmacological properties, functional features, and emerging specificities of the two major endocannabinoids. Mol. Neurobiol. 46 (2), 374–392. https://doi.org/10.1007/s12035-012-8299-0.

Malkova, N.V., Gallagher, J.J., Yu, C.Z., Jacobs, R.E., Patterson, P.H., 2014. Manganese-enhanced magnetic resonance imaging reveals increased DOI-induced brain activity in a mouse model of schizophrenia. Proc. Natl. Acad. Sci. U.S.A. 111 (24).

McCutcheon, J.E., Conrad, K.L., Carr, S.B., Ford, K.A., McGehee, D.S., Marinelli, M., 2012. Dopamine neurons in the ventral tegmental area fire faster in adolescent rats than in adults. J. Neurophysiol. 108 (6), 1620–1630. https://doi.org/10.1152/jn.00077.2012.

Melis, Miriam, Pistis, M., Perra, S., Muntoni, A. L., Pillolla, G., & Gessa, G. L. (2004). *Endocannabinoids Mediate Presynaptic Inhibition of Glutamatergic Transmission in Rat Ventral Tegmental Area Dopamine Neurons through Activation of CB1 Receptors*. *24*(1), 53–62. https://doi.org/10.1523/JNEUROSCI.4503-03.2004.

Melis, M., Pistis, M., 2007. Endocannabinoid Signaling in Midbrain Dopamine Neurons: More than Physiology? Curr. Neuropharmacol. 5 (4), 268–277. https://doi.org/10.2174/157015907782793612.

Melis, M., De Felice, M., Lecca, S., Fattore, L., Pistis, M., 2013. Sex-specific tonic 2-arachidonoylglycerol signaling at inhibitory inputs onto dopamine neurons of Lister hooded rats. Front. Integr. Neurosci. 7 (DEC), 1–13. https://doi.org/10.3389/fnint.2013.00093.

Melis, M., Sagheddu, C., Felice, M.D., Casti, A., Madeddu, C., Spiga, S., Muntoni, A.L., Mackie, K., Marsicano, G., Colombo, G., Castelli, M.P., Pistis, M., 2014. Enhanced endocannabinoid-mediated modulation of rostromedial tegmental nucleus drive onto dopamine neurons in sardinian alcohol-preferring rats. J. Neurosci. 34 (38), 12716–12724. https://doi.org/10.1523/JNEUROSCI.1844-14.2014.

Meyer, U., 2013. Developmental neuroinflammation and schizophrenia. Prog. Neuropsychopharmacol. Biol. Psychiatry 42, 20–34. https://doi.org/10.1016/j.pnpbp.2011.11.003.

Meyer, U., Feldon, J., Schedlowski, M., Yee, B.K., 2005. Towards an immuno-precipitated neurodevelopmental animal model of schizophrenia. Neurosci. Biobehav. Rev. 29 (6), 913–947. https://doi.org/10.1016/j.neubiorev.2004.10.012.

Meyer, H.C., Lee, F.S., Gee, D.G., 2018. The Role of the Endocannabinoid System and Genetic Variation in Adolescent Brain Development. Neuropsychopharmacology 43 (1), 21–33. https://doi.org/10.1038/npp.2017.143.

Meyer, U., Nyffeler, M., Yee, B.K., Knuesel, I., Feldon, J., 2008. Adult brain and behavioral pathological markers of prenatal immune challenge during early/middle and late fetal development in mice. Brain Behav. Immun. 22 (4), 469–486. https://doi.org/10.1016/j.bbi.2007.09.012.

Meyer, U., Weiner, I., McAlonan, G.M., Feldon, J., 2011. The neuropathological contribution of prenatal inflammation to schizophrenia. Expert Rev. Neurother. 11 (1), 29–32. https://doi.org/10.1586/ern.10.169.

Miller, A.H., Haroon, E., Raison, C.L., Felger, J.C., 2013. Cytokine targets in the brain: Impact on neurotransmitters and neurocircuits. Depress. Anxiety 30 (4), 297–306. https://doi.org/10.1002/da.22084.

Missault, S., Van den Eynde, K., Vanden Berghe, W., Fransen, E., Weeren, A., Timmermans, J.P., Kumar-Singh, S., Dedeurwaerdere, S., 2014. The risk for behavioural deficits is determined by the maternal immune response to prenatal immune challenge in a neurodevelopmental model. Brain Behav. Immun. 42 (2014), 138–146. https://doi.org/10.1016/j.bbi.2014.06.013.

Moore, K. W., Garra, A. O., Fiorentino, D. F., Zlotnik, A., Vieira, P., Mosmann, T. R., Howard, M., Moore, K. W., & Garra, A. O. (2016). *IL-10 acts on the antigen-presenting cell to inhibit cytokine production by Th1 cells . This information is current as Email Alerts Information about subscribing to The Journal of Immunology is online at : ON THE ANTIGEN-PRESENTING CELL TO INHIBIT CYTOKIN*. *6*.

Mueller, F.S., Polesel, M., Richetto, J., Meyer, U., Weber-Stadlbauer, U., 2018. Mouse models of maternal immune activation: Mind your caging system! Brain Behav. Immun. 73, 643–660. https://doi.org/10.1016/j.bbi.2018.07.014.

Murray, P.J., 2006. Understanding and exploiting the endogenous interleukin-10/STAT3-mediated anti-inflammatory response. Curr. Opin. Pharmacol. 6 (4), 379–386. https://doi.org/10.1016/j.coph.2006.01.010.

Pacheco-López, G., Giovanoli, S., Langhans, W., Meyer, U., 2013. Priming of metabolic dysfunctions by prenatal immune activation in mice: relevance to schizophrenia. Schizophr. Bull. 39 (2), 319–329. https://doi.org/10.1093/schbul/sbr178.

Paxinos, G., Watson, C., 2007. The rat brain in stereotaxic coordinates, 7th ed. Elsevier, London.

Pitler, T.A., Alger, B.A., 1994. Depolarization-induced suppression of GABAergic inhibition in rat hippocampal pyramidal cells: G protein involvement in a presynaptic mechanism. Neuron 13 (6), 1447–1455. https://doi.org/10.1016/0896-6273(94)90430-8.

Ramírez, B.G., Blázquez, C., Gómez Del Pulgar, T., Guzmán, M., De Ceballos, M.L., 2005. Prevention of Alzheimer's disease pathology by cannabinoids: Neuroprotection mediated by blockade of microglial activation. J. Neurosci. 25 (8), 1904–1913. https://doi.org/10.1523/JNEUROSCI.4540-04.2005.

Reisinger, S.N., Kong, E., Khan, D., Schulz, S., Ronovsky, M., Berger, S., Horvath, O., Cabatic, M., Berger, A., Pollak, D.D., 2016. Maternal immune activation epigenetically regulates hippocampal serotonin transporter levels. Neurobiol. Stress 4, 34–43. https://doi.org/10.1016/j.ynstr.2016.02.007.

Rockwell, C.E., Snider, N.T., Thompson, J.T., Vanden Heuvel, J.P., Kaminski, N.E., 2006. Interleukin-2 suppression by 2-arachidonyl glycerol is mediated through peroxisome proliferator-activated receptor γ independently of cannabinoid receptors 1 and 2. Mol. Pharmacol. 70 (1), 101–111. https://doi.org/10.1124/mol.105.019117.

Rom, S., Persidsky, Y., 2013. Cannabinoid receptor 2: Potential role in immunomodulation and neuroinflammation. J. Neuroimmune Pharmacol. 8 (3), 608–620. https://doi.org/10.1007/s11481-013-9445-9.

Santoni, M., Frau, R., Pistis, M., 2022. Transgenerational Sex-dependent Disruption of Dopamine Function Induced by Maternal Immune Activation. Front. Pharmacol. 13 (February), 1–10. https://doi.org/10.3389/fphar.2022.821498.

Scherma, M., Dessì, C., Muntoni, A.L., Lecca, S., Satta, V., Luchicchi, A., Pistis, M., Panlilio, L.V., Fattore, L., Goldberg, S.R., Fratta, W., Fadda, P., 2016. Adolescent Δ 9-Tetrahydrocannabinol Exposure Alters WIN55,212–2 Self-Administration in Adult Rats. Neuropsychopharmacology 41 (5), 1416–1426. https://doi.org/10.1038/npp.2015.295.

Shin, W.H., Lee, D.Y., Park, K.W., Kim, S.U., Yang, M.S., Joe, E.H., Jin, B.K., 2004. Microglia Expressing Interleukin-13 Undergo Cell Death and Contribute to Neuronal Survival in Vivo. Glia 46 (2), 142–152. https://doi.org/10.1002/glia.10357.

Sideromenos, S., Lindtner, C., Zambon, A., Horvath, O., Berger, A., Pollak, D.D., 2020. VEGF Treatment Ameliorates Depression-Like Behavior in Adult Offspring After Maternal Immune Activation. Cells 9 (4). https://doi.org/10.3390/cells9041048.

Stollenwerk, T.M., Hillard, C.J., 2021. Adolescent thc treatment does not potentiate the behavioral effects in adulthood of maternal immune activation. Cells 10 (12). https://doi.org/10.3390/cells10123503.

Sullivan, R., Wilson, D.A., Feldon, J., Yee, B.K., Meyer, U., Richter-Levin, G., Avi, A., Michael, T., Gruss, M., Bock, J., Helmeke, C., Braun, K., 2006. The International Society for Developmental Psychobiology annual meeting symposium: Impact of early life experiences on brain and behavioral development. Dev. Psychobiol. 48 (7), 583–602. https://doi.org/10.1002/dev.20170.

Talukdar, P.M., Abdul, F., Maes, M., Binu, V., Venkatasubramanian, G., Kutty, B.M., Debnath, M., 2020. Maternal Immune Activation Causes Schizophrenia-like Behaviors in the Offspring through Activation of Immune-Inflammatory, Oxidative and Apoptotic Pathways, and Lowered Antioxidant Defenses and Neuroprotection. Mol. Neurobiol. 57 (10), 4345–4361. https://doi.org/10.1007/s12035-020-02028-8.

Ungless, M.A., Grace, A.A., 2012. Are you or aren't you? Challenges associated with physiologically identifying dopamine neurons. Trends Neurosci. 35 (7), 422–430. https://doi.org/10.1016/j.tins.2012.02.003.

Van Den Eynde, K., Missault, S., Fransen, E., Raeymaekers, L., Willems, R., Drinkenburg, W., Timmermans, J.P., Kumar-Singh, S., Dedeurwaerdere, S., 2014. Hypolocomotive behaviour associated with increased microglia in a prenatal immune activation model with relevance to schizophrenia. Behav. Brain Res. 258 (2014), 179–186. https://doi.org/10.1016/j.bbr.2013.10.005.

Vuillermot, S., Weber, L., Feldon, J., Meyer, U., 2010. A longitudinal examination of the neurodevelopmental impact of prenatal immune activation in mice reveals primary defects in dopaminergic development relevant to schizophrenia. J. Neurosci. 30 (4), 1270–1287. https://doi.org/10.1523/JNEUROSCI.5408-09.2010.

Vuillermot, S., Feldon, J., Meyer, U., 2011. Nurr1 is not essential for the development of prepulse inhibition deficits induced by prenatal immune activation. Brain Behav. Immun. 25 (7), 1316–1321. https://doi.org/10.1016/j.bbi.2011.06.012.

Wastnedge, E.A.N., Reynolds, R.M., van Boeckel, S.R., Stock, S.J., Denison, F.C., Maybin, J.A., Critchley, H.O.D., 2021. Pregnancy and COVID-19. Physiol. Rev. 101 (1), 303–318. https://doi.org/10.1152/physrev.00024.2020.

Weber-Stadlbauer, U., Richetto, J., Zwamborn, R.A.J., Slieker, R.C., Meyer, U., 2021. Transgenerational modification of dopaminergic dysfunctions induced by maternal immune activation. Neuropsychopharmacology 46 (2), 404–412. https://doi.org/10.1038/s41386-020-00855-w.

Willi, R., Harmeier, A., Giovanoli, S., Meyer, U., 2013. Altered GSK3β signaling in an infection-based mouse model of developmental neuropsychiatric disease. Neuropharmacology 73, 56–65. https://doi.org/10.1016/j.neuropharm.2013.05.012.

Wu, X., French, E.D., 2000. Effects of chronic Δ9-tetrahydrocannabinol on rat midbrain dopamine neurons: An electrophysiological assessment. Neuropharmacology 39 (3), 391–398. https://doi.org/10.1016/S0028-3908(99)00140-9.

Yang, M.S., Park, E.J., Sohn, S., Kwon, H.J., Shin, W.H., Pyo, H.K., Jin, B., Choi, K.S., Jou, I., Joe, E.H., 2002. Interleukin-13 and -4 induce death of activated microglia. Glia 38 (4), 273–280. https://doi.org/10.1002/glia.10057.

Zamberletti, E., Gabaglio, M., Woolley-Roberts, M., Bingham, S., Rubino, T., Parolaro, D., 2019. Cannabidivarin Treatment Ameliorates Autism-Like Behaviors and Restores Hippocampal Endocannabinoid System and Glia Alterations Induced by Prenatal Valproic Acid Exposure in Rats. Front. Cell. Neurosci. 13 (August), 1–15. https://doi.org/10.3389/fncel.2019.00367.

Zhao, Q., Dai, W., Chen, H.Y., Jacobs, R.E., Zlokovic, B.V., Lund, B.T., Montagne, A., Bonnin, A., 2022. Prenatal disruption of blood-brain barrier formation via cyclooxygenase activation leads to lifelong brain inflammation. Proc. Natl. Acad. Sci. U.S.A. 119 (15), 1–12. https://doi.org/10.1073/pnas.2113310119.

Zuckerman, L., Rehavi, M., Nachman, R., Weiner, I., 2003. Immune activation during pregnancy in rats leads to a postpubertal emergence of disrupted latent inhibition, dopaminergic hyperfunction, and altered limbic morphology in the offspring: A novel neurodevelopmental model of schizophrenia. Neuropsychopharmacology 28 (10), 1778–1789. https://doi.org/10.1038/sj.npp.1300248.